# Key Determinants of Nucleotide-Activated G Protein-Coupled $P2Y_2$ Receptor Function Revealed by Chemical and Pharmacological Experiments, Mutagenesis and Homology Modeling

Petra Hillmann,[†] Geun-Yung Ko,[‡] Andreas Spinrath,[§] Alexandra Raulf,[†] Ivar von Kügelgen,[||] Samuel C. Wolff,[⊥] Robert A. Nicholas,[⊥] Evi Kostenis,[§] Hans-Dieter Höltje,[‡] and Christa E. Müller*[,†]

*PharmaCenter Bonn, Pharmaceutical Chemistry I, University of Bonn, An der Immenburg 4, 53121 Bonn, Germany, Department of Pharmacy, University of Düsseldorf, Universitätsstrasse 1, 40225 Düsseldorf, Germany, Institute for Pharmaceutical Biology, University of Bonn, Nussallee 6, 53115 Bonn, Germany, Department of Pharmacology, University of Bonn, Reuterstrasse 2b, 53113 Bonn, Germany, and Department of Pharmacology, The University of North Carolina at Chapel Hill, North Carolina 27599-7365*

*Received November 15, 2008*

The $P2Y_2$ receptor, which is activated by UTP, ATP, and dinucleotides, was studied as a prototypical nucleotide-activated GPCR. A combination of receptor mutagenesis, determination of its effects on potency and efficacy of agonists and antagonists, homology modeling, and chemical experiments was applied. R272 (extracellular loop EL3) was found to play a gatekeeper role, presumably responsible for recognition and orientation of the nucleotides. R272 is also directly involved in binding of dinucleotides, which behaved as partial agonists. Y118A (3.37) mutation led to dramatically reduced efficacy of agonists; it is part of the entry channel as well as the triphosphate binding site. While the Y114A (3.33) mutation did not have any effect on agonist activities, the antagonist Reactive Blue 2 (**6**) was completely inactive at that mutant. The disulfide bridge Cys25−Cys278 was found to be important for agonist potency but neither for agonist efficacy nor for antagonist potency.



## Introduction

G protein-coupled receptors are one of the largest families of proteins in the human genome (ca. 800 members), and they are the most important class of drug targets.[1] The largest subfamily of GPCRs[a] is the class A or rhodopsin receptor family (ca. 670 proteins).[2] The $P2Y_2$ receptor is a member of class A GPCRs and belongs to the family of nucleotide-activated P2 receptors. These are divided into two subfamilies: P2Y receptors (P2YR), which are GPCRs, and P2X receptors, which form ligand-gated ion channels.[3] So far, the P2YR subfamily consists of eight members: $P2Y_1$, $P2Y_2$, $P2Y_4$, $P2Y_6$, $P2Y_{11}$, $P2Y_{12}$, $P2Y_{13}$, and $P2Y_{14}$, which can be subgrouped into $P2Y_1$-like, $G_q$ protein-coupled receptors ($P2Y_{1,2,4,6,11}$), and $P2Y_{12}$-like, $G_{i/o}$-coupled receptors ($P2Y_{12,13,14}$).[4] In contrast to the ATP (adenosine-5′-triphosphate (**1**)-activated P2X receptors, the P2YR subtypes are differentially activated by physiological nucleotides: human $P2Y_1$ (ADP (adenosine-5′-diphosphate)), $P2Y_6$ (UDP (uridine-5′-diphosphate)), $P2Y_{12}$ (ADP), and $P2Y_{13}$ (ADP) receptors are activated by nucleoside diphosphates, and $P2Y_{14}$ by UDPglucose, while $P2Y_2$ (ATP, UTP), $P2Y_4$ (UTP), and $P2Y_{11}$ (ATP) receptors require nucleoside triphosphates for activation. The $P2Y_2R$ is a special receptor because it represents a link between the adenine ($P2Y_1$, $P2Y_2$, $P2Y_{11-13}$) and the pyrimidine ($P2Y_{2,4,6,14}$) nucleotide-activated receptor subtypes: it can be stimulated by both ATP and UTP with similar potency and efficacy. Furthermore, dinucleotides such as diadenosine tetraphosphate ($Ap_4A$ (**2**)) or diuridine tetraphosphate ($Up_4U$ (**5**)) can also potently activate $P2Y_2R$ and may be physiological agonists as well.[5] Thus, the $P2Y_2$ receptor is highly promiscuous toward various physiological agonists and studying its interaction with the structurally diverse ligands could also provide general insights into the interaction of GPCRs with their ligand, and especially with nucleotides and perhaps other anionic ligands.

$P2Y_2R$ are widely distributed in the human body, showing particularly high expression on immune cells, epithelial and endothelial cells, kidney tubules, and osteoblasts.[6] They appear to be involved in a number of physiological as well as pathological mechanisms.[7] Activation of the receptors leads to vasodilatation[8] and in epithelial tissue to chloride secretion and therefore hydration on epithelial layers.[9] Furthermore, the $P2Y_2R$ is coupled to pro-inflammatory signaling pathways[10] and it may inhibit neurodegeneration.[11] $P2Y_2R$ can modulate cell proliferation and regulate the cell cycle.[12,13] Because of these functions, the $P2Y_2R$ is an intriguing novel drug target. In fact, $P2Y_2R$ agonists with dinucleotide structure ($Up_4U$ or diquafosol (**5**) and denufosol (2′-desoxycytidin(5′)tetraphospho(5′)uridin)) are currently undergoing clinical trials as novel treatments for dry eye syndrome or cystic fibrosis, respectively.[14,15] However, potency, efficacy, and selectivity of these dinucleotides are only moderate, and although they are metabolically more stable than mononucleotides such as ATP and UTP, the dinucleotides typically suffer from relatively short half-lives due to enzymatic hydrolysis, especially by nucleotide pyrophosphatases (NPPs).[16] Potent and selective agonists and antagonists are required to learn more about the (patho)physiological roles of these receptors and to explore their therapeutic potential. However, it appears to be quite difficult to develop selective ligands for $P2Y_2R$ as well as for some other P2YR subtypes.[17]

* To whom correspondence should be addressed. Phone: +49-228-73-2301. Fax: +49-228-73-2567. E-mail: christa.mueller@uni-bonn.de.
[†] PharmaCenter Bonn, Pharmaceutical Chemistry I, University of Bonn.
[‡] Department of Pharmacy, University of Düsseldorf.
[§] Institute for Pharmaceutical Biology, University of Bonn.
[||] Department of Pharmacology, University of Bonn.
[⊥] Department of Pharmacology, The University of North Carolina at Chapel Hill.

[a] Abbreviations: GPCR, G protein-coupled receptor; P2YR, P2Y receptor; $Ap_4A$ diadenosine tetraphosphate; $Up_4U$, diuridine tetraphosphate; NPP, nucleotide pyrophosphatases; RB2 Reactive Blue 2; TM, transmembrane helix; EL, extracellular loop; NT, N-terminus; HA, hemagglutinin; VSV-G, vesicular stomatitis virus G protein; PB, phosphate-buffered saline; wt, wild type; $[Ca^{2+}]_i$, intracellular calcium concentration; MD simulation, molecular dynamic simulation; $EC_{50}$, half-maximal effective concentration; $IC_{50}$, half-maximal inhibitory concentration.

10.1021/jm801442p CCC: $40.75 
Published on Web 04/01/2009

Regarding agonists, a few UTP analogues such as 2-thio-2′-amino-2′deoxy-UTP and 2-thio-UTP have been synthesized that show some selectivity for the $P2Y_2R$;[18,19] however, such compounds will hardly be "druggable" due to their presumed physiological instability toward phosphatases. Increased metabolic stability of nucleotides may be achieved by modification of the phosphate ester chain, e.g., by boranophosphates,[20,21] by replacement of the $\beta,\gamma$-oxygen atom by a dihalogenomethylene bridge[18,22] or by the dinucleotide approach as in $Up_4U$.[17,23] So far, however, no potent and highly selective agonist has been obtained in these series of compounds. Classical $P2Y_2$ antagonists comprise the moderately potent, nonselective sulfonates Reactive Blue 2 (RB2 (**6**))[24] and suramin (**7**).[25] Recently, truncated derivatives of **6** like 1-amino-4-(4-methoxyphenyl)-2-sulfoanthraquinone (PSB-416 (**8**)) have been found to be equally potent and somewhat more selective $P2Y_2R$ antagonists.[26]

To fundamentally understand the interactions of the human $P2Y_2R$ as a prototypic nucleotide-activated GPCR with its ligands, we chose an approach combining (i) site-directed mutagenesis, (ii) pharmacological experiments applying structurally diverse ligands (various agonists and antagonists), (iii) chemical experiments utilizing a disulfide-reducing reagent, and (iv) receptor homology modeling.

So far only three amino acids (H262, R265, and R292, which correspond to 6.52, 6.55, and 7.39, respectively in the Ballesteros−Weinstein nomenclature[27]) in the sixth and seventh transmembrane helices (TM6, TM7) have been shown to be part of the potential UTP/ATP binding site in the $P2Y_2$ receptor,[28] suggesting that these basic residues interact with the negatively charged phosphate chain of the nucleotides. Another basic residue, K289 (7.54) in TM7, had no effect on agonist activation, but its mutation to arginine increased the activity of diphosphates (ADP and UDP). An important role of basic amino acids in the same positions of TM6 (6.52, 6.55) and TM7 (7.39) was also found for $P2Y_1$ and $P2Y_{11}$ receptors; in addition, a basic arginine residue in TM3 (3.29) proved to be essential for receptor activation of both $P2Y_1$ and $P2Y_{11}$ receptors and was postulated to interact with a nucleotide phosphate group.[29−31]

Site-directed mutagenesis of the $P2Y_4R$, which is most closely related to $P2Y_2R$ (41% overall sequence identity), showed an important role for several amino acid residues in the second extracellular loop (EL2) on effects of ATP, which is an antagonist at the human but an agonist at the rat receptor.[32] The most extensive mutagenesis studies have been performed on the $P2Y_1$ receptor, showing the crucial importance of several amino acids in the extracellular loops (EL1, EL2, and EL3).[4,29,33] However, it is not clear whether these results apply to $P2Y_2$ receptors as well and whether they are of general significance for the P2Y receptor family and other GPCRs.

Coupling of the $P2Y_2R$ to integrins and apical targeting induced by $P2Y_2R$ activation was prevented by mutating the R95, G96, D97 (RGD) consensus sequence in the first extracellular loop into RGE.[34] In addition, L108 in the first extracellular loop was important for apical targeting.[35] The $P2Y_2$ receptor shows agonist-induced internalization,[36,37] which is influenced by phosphorylation sites in the C-terminus and the third intracellular loop (S243, T344, S356).[38] A model of the $P2Y_2$ receptor suggesting putative binding sites for agonists, but not for antagonists, has been published by Ivanov, Jacobson et al.[19,39] It was based on data from the few mutagenesis studies published so far for $P2Y_2R$ as well as structure−activity relationships of a series of agonists derived from the physiological nucleotide UTP.

In the present study, we provide evidence that the function of the $P2Y_2$ receptor is dependent on interactions of ligands with amino acid residues in TM3, 5, and 7 as well as in the EL2 and 3. Furthermore mutagenesis and chemical reduction experiments show dependence on two conserved disulfide bridges in the receptor protein. Our new $P2Y_2R$ homology model is well in accordance with the experimental data and offers novel information about ligand recognition and binding by the receptor. Such information will serve as a basis for the future design of new ligands for the $P2Y_2R$ and may even prove useful for other nucleotide receptors and related members of the GPCR family.

## Results

**Site-Directed Mutagenesis.** The human $P2Y_2$ receptor, harboring a HA epitope sequence at the N-terminus, was cloned into the retroviral expression vector pLXSN. The following mutations were introduced (Figure 1): (a) C106 (EL1), which can form a disulfide bridge with C183 (EL2), and C278 (EL3), which purportedly forms a disulfide bridge with C25 (N-terminus, NT), were homologously replaced by serine; (b) Y114A (3.33), Y118A (3.37), Y198A (5.38), and S296A (7.43), all of which were selected based on a preliminary receptor homology model, which indicated that they may line the ligand-binding site; and (c) R177A, R180A, R194H (in EL2), and R272A (EL3), including an R177A_R180A double mutant; these basic amino acids in the extracellular loops are predicted to be involved in binding of the negatively charged nucleotides. Figure 1 shows a snake-like plot of the receptor sequence indicating the mutated amino acid residues.

**Receptor Expression and Cell Surface ELISA.** The wild-type receptor and the mutants were stably expressed in 1321N1 astrocytoma cells using a retroviral expression system. The wild-type receptor was shown to be functional. The physiological agonists UTP and ATP led to a concentration-dependent increase in the intracellular calcium concentration as shown in Figure 2A for UTP. Nontransfected 1321N1 cells did not respond to UTP or ATP (not shown).

Almost all mutants could be detected on the cell surface as determined by whole cell ELISA assays (Figure 2B). Only the mutant C106S could not be detected, indicating that the disulfide bridge between C106 and C183 is crucial for the tertiary structure of the receptor protein. The expression levels of the other receptor mutants showed some variations, ranging from about 40% to about 150% with respect to the highest expressing wild-type cell line (Figure 2B). Because the expression level will influence the $EC_{50}$ values of agonists in functional assays,[54,55] we prepared stable wild-type cell lines that showed different expression levels (named wt1−wt4). This was achieved by varying the transfection conditions using different virus titers, amounts of DNA, or packaging cells. Three wild-type cell lines, wt1, wt3, and wt4, were further evaluated and $EC_{50}$ values for UTP were determined in calcium mobilization assays (Figure 2C). The cell line wt2 was not significantly different from wt3 (not shown).

$P2Y_2$ receptor cell lines with expression levels of 100% (wt4) and 52% (wt3) did not show large differences in their $EC_{50}$ values (Figure 2C), while the cell line wt1, which showed only 14% of the level of expression of receptor compared to wt4, had an $EC_{50}$ value that was about 1 order of magnitude higher for all agonists investigated. Thus we divided the cell lines expressing the mutant receptors into two groups: the first one exhibiting expression levels between 82% and 154%, and the second group between 39% and 68% (Figure 2B). In each group,

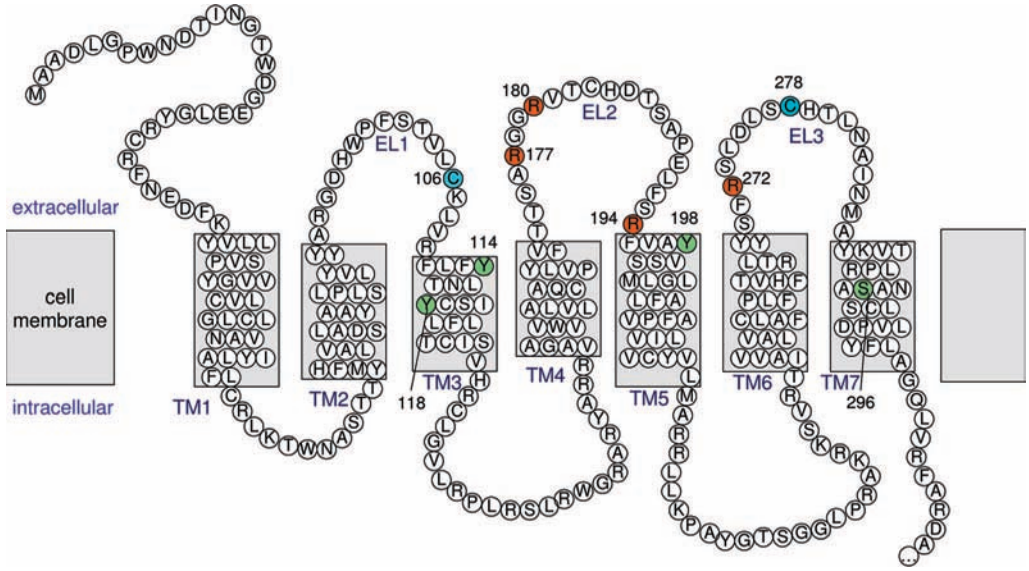


**Figure 1.** Snake-like plot of the human $P2Y_2$ receptor (C-terminus truncated). In the extracellular loops, EL2 and EL3 positively charged amino acids were mutated: the double mutant R177A_R180A, the corresponding single mutants R177A and R180A, as well as R194H were introduced into the second extracellular loop; R272 was mutated to alanine in the third extracellular loop. In the third, fifth, and seventh transmembrane helices, the following mutations were generated: Y114A, Y118A, Y198A, and S296A. As parts of putative disulfide bridges, two cysteine residues were homologously exchanged for serine: C106S and C278S.



the potency and efficacy of the agonists and antagonists was compared with the corresponding wild-type cell line (wt3 or wt4, respectively).

**Investigated Ligands.** To characterize the $P2Y_2$ receptor mutants, intracellular calcium measurements were performed. At each stably transfected wild type and mutant cell line, the physiological nucleotides UTP and ATP, as well as the dinucleotides $Ap_4A$ (with identical nucleobases) and $Ip_4U$ (with different nucleobases), were investigated (Figure 3).

The results were set in relation to the effects of 100 $\mu$M **9**, which was used as an internal standard (set at 100%) due to its activation of natively expressed $G_q$-coupled M3 muscarinic receptors. UTP and ATP induced $P2Y_2$-mediated intracellular calcium release, with $EC_{50}$ values of 59 nM (UTP) and 63 nM (ATP). Maximal increases in intracellular calcium concentration were slightly higher than those determined for **9** (UTP 138%, ATP 110%). The dinucleotides $Ap_4A$ and $Ip_4U$ were potent agonists at the $P2Y_2$ receptor. In general, their $EC_{50}$ values (167 nM for $Ap_4A$ and 179 nM for $Ip_4U$) were slightly lower than those observed for ATP and UTP. Furthermore, lower efficacies were observed for the dinucleotides in comparison with the mononucleotides.

In addition, two different antagonists, the relatively large molecule **6** and the small molecule **8** (for structures see Figure 3), were investigated for their potential to inhibit UTP-induced calcium mobilization. Both anthraquinone derivatives showed antagonistic effects at the $P2Y_2$ receptor in the low micromolar range (Table 2). $IC_{50}$ values were determined to be 1.85 $\mu$M for **6** and 21.7 $\mu$M for **8** using a concentration of 0.5 $\mu$M UTP for receptor stimulation.

**Chemical Reduction of Disulfide Bridges.** To investigate the role of potential disulfide bridges for $P2Y_2$ receptor activation, the 1321N1 astrocytoma cells stably expressing the human $P2Y_2$ receptor (cell line wt1) were assayed for activation by UTP and ATP under reducing conditions. Intracellular calcium levels were determined after preincubation with 1,4-dimercapto-2,3-butandiol, Butan-2,3-diol-1,4-dithiol, dithiothreitol (DTT) (1 mM or 10 mM, respectively, Figure 4).

Stimulation of the muscarinic M3 receptor with the agonist **9** was used as a reference. DTT pretreatment led to a small decrease in the M3 receptor response (from 100% to 79%) upon application of a high concentration of **9** (100 $\mu$M). DTT pretreatment has also been shown to mediate a reduction in antagonist binding affinity by 20% at rat muscarinic receptors.[56] The activation of the $P2Y_2R$ was affected to a much larger extent. A significant reduction in receptor activation, i.e., 80 $\pm$ 15% or 74 $\pm$ 5% for UTP (1 or 10 $\mu$M) and 91 $\pm$ 17% or 81 $\pm$ 6% for ATP (1 or 10 $\mu$M) was observed due to chemical reduction of disulfide bridges ($n = 3$). This effect was reversible (data not shown).

**Characterization of Cysteine Mutants.** The $P2Y_2$ receptor mutant C278S expressed in 1321N1 astrocytoma cells was investigated for its ability to be activated by the nucleotides UTP and ATP as well as by the dinucleotides $Ap_4A$ and $Ip_4U$ (Figure 5, Table 1). Intracellular calcium release was monitored and compared with the increases in $[Ca^{2+}]_i$ induced by **9** (100 $\mu$M). The mutation C278S caused a significant increase in $EC_{50}$ values for UTP (25-fold), ATP (10-fold), $Ap_4A$ (about 560-fold), and $Ip_4U$ (about 2400-fold) compared to the wild-type receptor (wt3) but did not completely prevent receptor activation (Table 1). The efficacy of the nucleotides appeared not to be affected by preventing the formation of the disulfide bridge C25−C278. Figure 5 shows concentration−response curves for UTP, ATP, $Ap_4A$, and $Ip_4U$ at the wt3 and the $P2Y_2$ receptor mutant C278S. As a next step, the cells were preincubated with the antagonists **6** and **8** and subsequently stimulated with UTP at a concentration leading to 80−90% of the maximal effect (Table 1). Compound **6** showed no significant difference in $IC_{50}$ values (wt1, 1.62 $\mu$M; C278S 1.05 $\mu$M), whereas for **8**, the concentration−response curve was shifted to the left ($IC_{50}$ of 3.44 $\mu$M compared to 21.9 $\mu$M at the wild-type $P2Y_2R$).

**Mutations of Tyrosine and Serine Residues in Helices 3, 5, and 7.** At the Y114A (3.33) mutant, the nucleotides showed activation in the same range as at the wild-type receptor (wt4) (Table 2, Figures 6, 7). The mutation Y118A (3.37) led to a 2-fold (but nonsignificant) increase in the $EC_{50}$ value of UTP and significantly increased the $EC_{50}$ value of ATP (3-fold). In

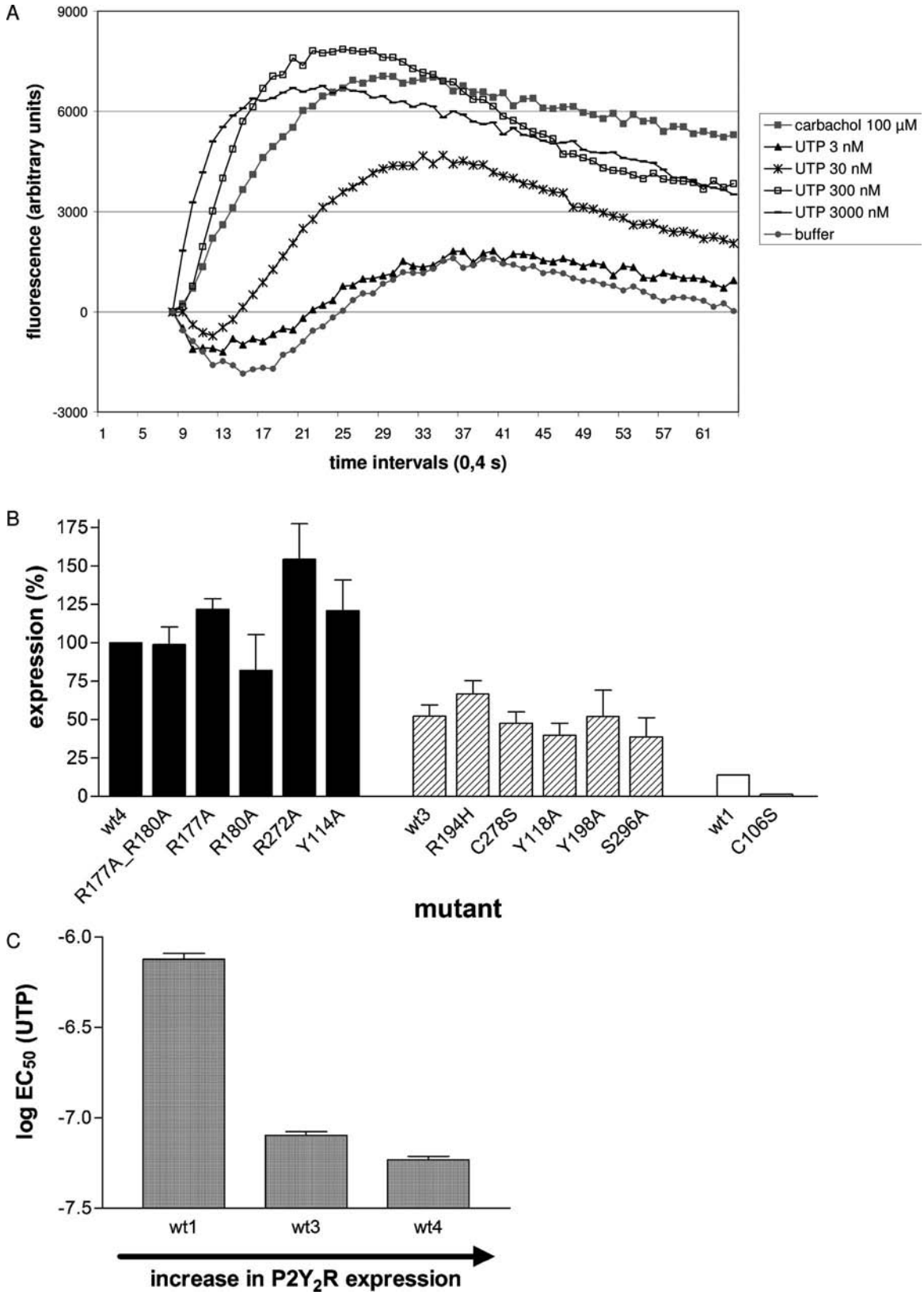


**Figure 2.** (A) Analysis of intracellular calcium concentrations in 1321N1 cells after stimulation of the wild-type P2Y$_2$R. Cells were loaded with the calcium-sensitive dye Oregon Green BAPTA-1/AM, and different concentrations of UTP were injected to the cell suspension. Changes in fluorescence were determined. Concentration-dependent increases in $[Ca^{2+}]_i$ could be detected that were similar to those obtained after addition of the muscarinic M3 receptor agonist carbachol (**9**) (100 $\mu$M). Representative experiments of $n = 3$. (B) Expression rates of the receptor mutants determined by a cell surface ELISA with antibodies directed against the N-terminal HA-tag ($n = 3-8$). Except for C106S, all mutants were expressed in 1321N1 astrocytoma cells. Expression was set in relation to the wild-type cell line wt4 (100% expression). The mutants were assigned to three groups depending on the expression level and compared with data obtained with a wild-type cell line expressing similar levels of receptors. (C) $EC_{50}$ values for UTP determined in calcium mobilization assays at 1321N1 astrocytoma cell lines expressing the wild-type P2Y$_2$ receptor at different expression levels (wt1, 14%; wt3, 52%; wt4, 100%). In cells expressing wild-type receptors at 100% or 52%, respectively, $EC_{50}$ values for UTP were similar (59.0 $\pm$ 4.6 nM vs 80.4 $\pm$ 6.4 nM). When the expression rate amounted to only 14%, the $EC_{50}$ was considerably higher (781 $\pm$ 113 nM) ($n = 3-4$).

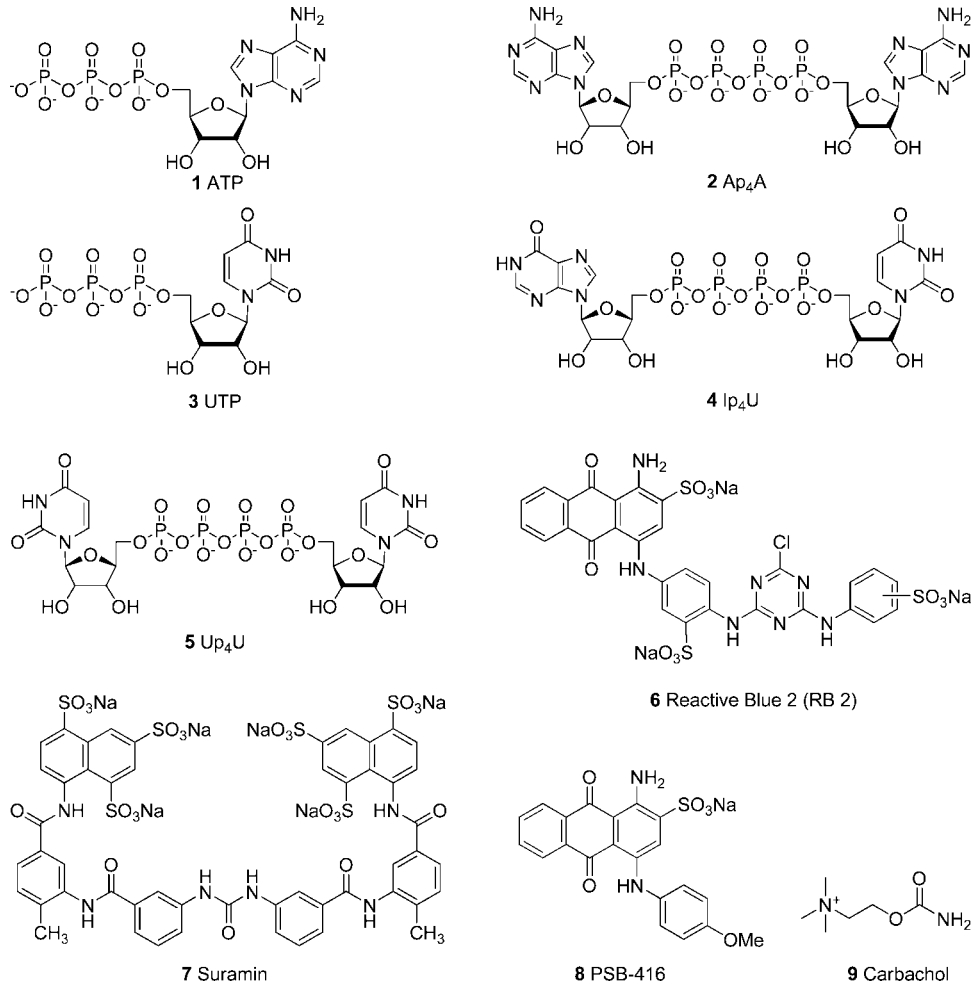


**Figure 3.** Structures of investigated $P2Y_2$ receptor agonists and antagonists and reference compound carbachol.

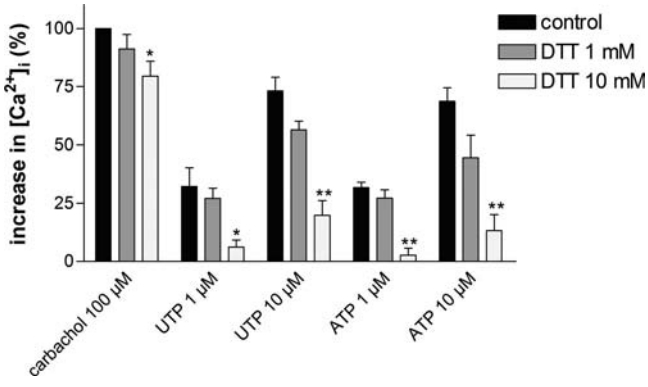


**Figure 4.** Effects of chemical reduction of disulfide bridges in the human $P2Y_2R$ on UTP-induced calcium mobilization. 1321N1 astrocytoma cells stably transfected with the $P2Y_2R$ were loaded with the calcium-sensitive dye Oregon Green BAPTA-1/AM and preincubated with DTT (dithiothreitol; 1 mM or 10 mM) for 15 min. UTP and ATP (1 $\mu$M and 10 $\mu$M) as well as the M3 receptor agonist **9** (100 $\mu$M) were added to the cells and $[Ca^{2+}]_i$ was determined. Calcium increases after addition of **9** were set at 100%. The **9** effect was slightly reduced by 20 ± 11% after DTT treatment. Responses to stimulation of $P2Y_2R$ were strongly affected by disulfide bridge reduction. For UTP, receptor activation was decreased by 80 ± 15% (1 $\mu$M) and 74 ± 5% (10 $\mu$M), respectively. Activation by ATP was reduced by 91 ± 17% (1 $\mu$M) and 81 ± 6%, respectively ($n = 3$); * $p < 0.05$; ** $p < 0.01$.

addition, it reduced the efficacy of both nucleotides by ca. 50%. The $EC_{50}$ value for $Ap_4A$ was also increased from 145 to 345 nM, and the efficacy was dramatically reduced (Table 2). For $Ip_4U$, only a minor increase in $EC_{50}$ was found but the efficacy was similarly reduced as with $Ap_4A$.

The mutant Y198A (5.38) did not show any significant difference in $EC_{50}$ values compared with the wild-type receptor (Table 2); it only showed a slightly increased efficacy for $Ap_4A$ and $Ip_4U$.

In contrast, mutation of S296 (7.43) to alanine led to a complete loss of receptor function for all agonists investigated.

The activatable mutants were further investigated with respect to the activity of two different antagonists, **6** and **8**. Compound **6** exhibited an $IC_{50}$ value of 1.85 $\mu$M at the wild-type receptor (Table 3, Figure 8). These data are in accordance with literature values for the wild-type $P2Y_2R$.[17] At the mutant Y118A receptor a similar $IC_{50}$ value was determined. In contrast, **6** was inactive at the Y114A mutant, and the concentration−response curve was significantly shifted to the right for the Y198A mutant receptor (from an $IC_{50}$ of 1.62 $\mu$M to 9.30 $\mu$M). The much smaller antagonist **8** behaved differently because it was equally potent at the wild-type and the Y118A, Y114A, and Y198A mutant receptors (Table 3).

**Mutations of Arginine Residues in the Extracellular Loops EL2 and EL3.** The double mutant R177A_R180A (EL2) led to a rightward shift of the concentration−response curve for the agonists ATP and UTP (Table 2, Figure 6A,B), most pronouncedly for ATP (wt4: $EC_{50}$ ATP = 63 nM; R177A_R180A: $EC_{50}$ ATP = 239 nM, 4-fold shift). For the dinucleotides $Ap_4A$ and $Ip_4U$, no significant rightward shift was determined (Figure 7). Subsequently, the effects of the single mutants R177A and

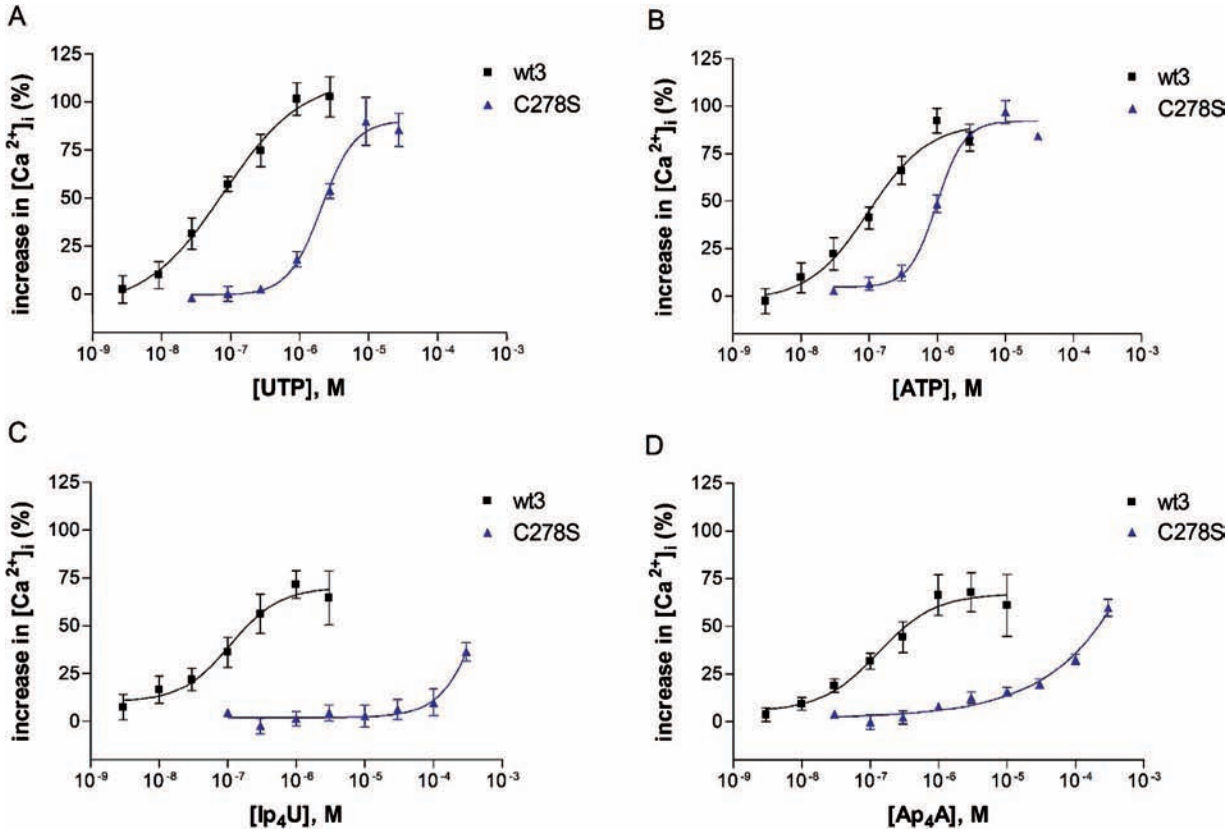


**Figure 5.** Agonist activation of the wild-type P2Y$_2$ receptor (wt3) and the P2Y$_2$ mutant C278S. 1321N1 astrocytoma cells expressing the wild-type receptor (wt3) or the mutant C278S were assayed for intracellular calcium release after addition of different concentrations of (A) UTP, (B) ATP, (C) Ap$_4$A, and (D) Ip$_4$U. For EC$_{50}$ values, see Table 1 ($n = 4$).

**Table 1.** EC$_{50}$/IC$_{50}$ Values for the P2Y$_2$ Receptor wt3 and for C278S Expressed in 1321N1 Astrocytoma Cells[a]

| | wt3 | | C278S | | |
|---|---|---|---|---|---|
| compd | EC$_{50}$ or IC$_{50}$ ($\mu$M ± SEM) | efficacy[b] (% ± SEM) | EC$_{50}$ or IC$_{50}$ ($\mu$M ± SEM) | efficacy[b] (% ± SEM) | fold shift[c] |
| UTP | 0.0804 ± 0.0064 | 100 ± 13 | 2.09 ± 0.32**[g] | 86 ± 9 | 25 |
| ATP | 0.0958 ± 0.0145 | 92 ± 6 | 1.00 ± 0.10***[h] | 97 ± 6 | 10 |
| Ap$_4$A | 0.145 ± 0.023 | 68 ± 8 | ca. 81[d] | n.a.[e] | 560 |
| Ip$_4$U | 0.112 ± 0.017 | 60 ± 5 | ca. 270[d] | n.a.[e] | 2400 |
| **6** | 1.62 ± 0.27 | | 1.05 ± 0.22 | | 0.6 |
| **8** | 21.9 ± 3.9 | | 3.44 ± 0.61*[f] | | 0.2 |

[a] Efficacy was determined in comparison to 100 $\mu$M **9**. For significantly shifted concentration−response curves, the shift of the EC$_{50}$/IC$_{50}$ value was calculated ($n = 3-4$). [b] Compared with 100 $\mu$M **9** (100%). [c] EC$_{50}$ or IC$_{50}$ of mutant divided by EC$_{50}$ or IC$_{50}$ of wild type. [d] Estimated by extrapolation of the concentration−response curve. [e] Up to 300 $\mu$M concentration no plateau was reached. [f] *: $p < 0.05$. [g] **: $p < 0.01$. [h] ***: $p < 0.001$.

R180A were investigated (Table 2, Figures 6, 7). Both mutants led to increased EC$_{50}$ values for agonists, but the effect of R180A was clearly stronger than that of R177A.

The mutant R194H did not show any significant difference in EC$_{50}$ values compared with the wild-type receptor (Figures 6C,D, 7C,D). Nevertheless, R194H showed significantly higher efficacies of 127% for UTP and 130% for ATP compared to 100% and 92% for the wild-type receptor wt3. The R194H mutant also exhibited a 2-fold higher efficacy for Ap$_4$A and a slightly increased efficacy for Ip$_4$U.

The positively charged R272 in EL3 strongly affected receptor activation (Table 2). Curves for all four agonists investigated were significantly shifted to the right in the R272A mutant (UTP: 350-fold; ATP: 185-fold) (Figure 6A,B). For dinucleotides, no plateau was reached at concentrations of up to 300 $\mu$M. Increases in the EC$_{50}$ value of more than 3 orders of magnitude for Ap$_4$A and Ip$_4$U can be estimated (Figure 7A,B).

Compound **6** exhibited an IC$_{50}$ value of 1.85 $\mu$M at the wild-type receptor, and similar IC$_{50}$ values were determined at the mutants R177A, R180A, Y118A, and R194H (Table 3, Figure 8A,C). However, mutations of the basic amino acid residues in EL2 led the inability of **6** to completely inhibit UTP activation of the P2Y$_2$R (~55%). At the double mutant R177A_R180A, **6** was 10-fold less potent than at the wild-type receptor. In contrast, the IC$_{50}$ value of the smaller antagonist **8** was not influenced by the mutations of the basic amino acids in EL2 (Figure 8B).

**Homology Modeling and Docking Studies.** A model of the P2Y$_2$R was generated in homology to the crystal structure of bovine rhodopsin. This GPCR has a slightly higher overall sequence identity to the human P2Y$_2$R than the recently crystallized $\beta$2 adrenergic receptor.[50,51] A molecular dynamics (MD) simulation (MD simulations not shown) was performed in a virtual membrane comprising a lipid bilayer and an aqueous phase. Two extracellular disulfide bridges between cysteine residues C25 and C278, which are highly conserved in GPCRs, as well as between C106 and C183, which are conserved in P2Y receptors, were proposed (Figure 9A).

Binding sites for UTP, ATP, and dinucleotides were identified (Figure 9B,C,D and Supporting Information). A binding pocket could be determined in the upper third part of the receptor molecule (Figure 9F). An entry channel between TM5 and TM6 was found to lead to this binding site (Figure 9G). This channel also provides a binding pocket for larger ligands like dinucleotides. Ionic, lipophilic, $\pi-\pi$, and hydrogen bonding interactions between the residues in the binding site and agonists were identified. Binding of ATP and UTP led to an induced fit of

**Table 2.** Agonist Stimulation of the Human $P2Y_2$ Receptor and Its Mutants[a]

| | UTP | | ATP | | $Ap_4A$ | | $Ip_4U$ | |
|---|---|---|---|---|---|---|---|---|
| wt or mutant | $EC_{50}$ ± SEM(nM) | efficacy (% ± SEM)[b] | $EC_{50}$ ± SEM(nM) | efficacy (% ± SEM)[b] | $EC_{50}$ ± SEM(nM) | efficacy (% ± SEM)[b] | $EC_{50}$ ± SEM(nM) | efficacy (% ± SEM)[b] |
| wt4 | 59.0 ± 4.6 | 138 ± 10 | 63.1 ± 8.2 | 110 ± 15 | 167 ± 60 | 100 ± 6 | 179 ± 55 | 98 ± 9 |
| Y114A | 37.2 ± 9.0 | 107 ± 9 | 30.1 ± 4.8*[f] | 87 ± 14 | 170 ± 42 | 128 ± 16 | 94.5 ± 6.5 | 142 ± 8*[f] |
| R177A_R180A | 123 ± 40 | 109 ± 9 | **239 ± 28*****[h] | 104 ± 10 | 665 ± 420 | 98 ± 5 | 398 ± 213 | 101 ± 7 |
| R177A | 50.1 ± 17.7 | 133 ± 8 | **183 ± 46***[f] | 117 ± 8 | 1230, 1690*[e f] | 86, 121[e] | 572 ± 145 | 102 ± 0 |
| R180A | 138 ± 21*[f] | 130 ± 24 | **237 ± 47****[g] | 115 ± 13 | 423 ± 140 | 68 ± 11 | 419 ± 131 | 72 ± 11 |
| R272A | **20600 ± 5000***[f] | **99 ± 6***[f] | **11700 ± 4400***[f] | **87 ± 6***[f] | ca. **740000**[c] | na[d] | ca. **620000**[c] | na[d] |
| wt3 | 80.4 ± 6.4 | 100 ± 13 | 95.8 ± 14.5 | 92 ± 6 | 145 ± 23 | 68 ± 8 | 112 ± 17 | 72 ± 7 |
| Y118A | 157 ± 49 | **43 ± 4****[g] | **299 ± 49****[g] | **41 ± 4****[g] | **345 ± 44****[g] | **15 ± 3****[g] | 145 ± 47 | **25 ± 5****[g] |
| R194H | 121 ± 54 | **127 ± 33***[f] | 111 ± 85 | **130 ± 11***[f] | 185 ± 9 | **149 ± 11****[g] | 216 ± 56 | 85 ± 10 |
| Y198A | 108 ± 38 | 128 ± 8 | 120 ± 32 | 126 ± 8*[f] | 335 ± 216 | 117 ± 11*[f] | 231 ± 45 | 127 ± 4*[f] |
| S296A | ≫ **300000** | **3 ± 1*****[h] | ≫ **300000** | **5 ± 2*****[h] | ≫ **300000** | **12 ± 1*****[h] | ≫ **300000** | **5 ± 2*****[h] |

[a] Increases in intracellular calcium concentrations were measured and $EC_{50}$ values as well as the maximal responses (efficacies) were determined. Values were set in relation to effects of the muscarinic M3 receptor agonist **9** (100 $\mu$M). Stably expressed mutant receptors were compared with the corresponding wild type receptor that showed a similar expression level (wt3 or wt4) ($n = 3-6$). [b] Compared with the effect induced by 100 $\mu$M **9**. [c] Estimated by extrapolation of the concentration−response curve. [d] At concentrations up to 300 $\mu$M no plateau was reached. [e] $n = 2$. [f] *: $p < 0.05$. [g] **: $p < 0.01$. [h] ***: $p < 0.001$ (*t* test).

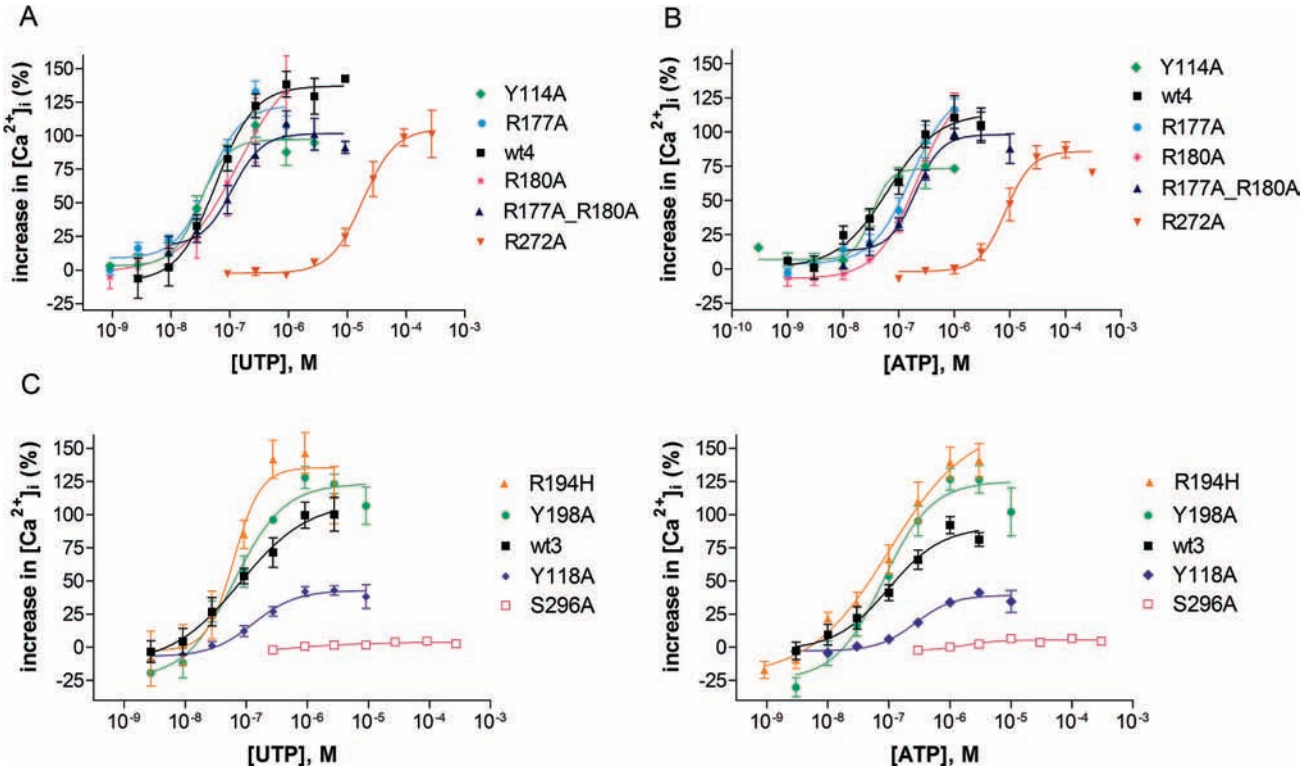


**Figure 6.** Activation of $P2Y_2R$ mutants by UTP and ATP in comparison to the wt $P2Y_2R$ (wt4 and wt3) stably expressed in 1321N1 astrocytoma cells ($n = 3-6$). (A) UTP stimulation of highly expressed mutants. (B) ATP stimulation of highly expressed mutants. (C) UTP stimulation of mutants with intermediate expression rates. (D) ATP stimulation of mutants with intermediate expression rates.

the receptor protein (Figure 9E). UTP induced a larger protein rearrangement than ATP because the protein had to adapt itself more strongly to the smaller UTP molecule, resulting in the formation of more stable hydrogen bonds in the UTP−$P2Y_2$ complex compared to that of the ATP−$P2Y_2$ complex.

In the present study, antagonist docking and MD simulation studies were performed at the $P2Y_2$ receptor for the first time. The two selected competitive antagonists **6** and **8** bind to the same interaction site as agonist ligands (Figure 9D). However, the antagonists are interacting with different amino acids (Supporting Information Figure 4). Some of the amino acids mutated in the present study were suggested to participate in ligand binding by the model (Figure 9 and Supporting Information), and vice versa, the model could be refined by the experimental results.

## Discussion

The $P2Y_2$ receptor is a promising target for the development of novel drugs, e.g., for the treatment of cystic fibrosis, dry eye syndrome, atherosclerosis, and neurodegenerative diseases.[14,34,57,58] It has been a major challenge to develop potent, selective, and metabolically stable agonists for this receptor subtype.[3,17] Potent and selective $P2Y_2$ antagonists are currently not available but would be highly desirable for studying the (patho)physiological roles of the $P2Y_2R$. Therefore, insights into the structure of the binding pocket and the mechanism of receptor binding and activation provide

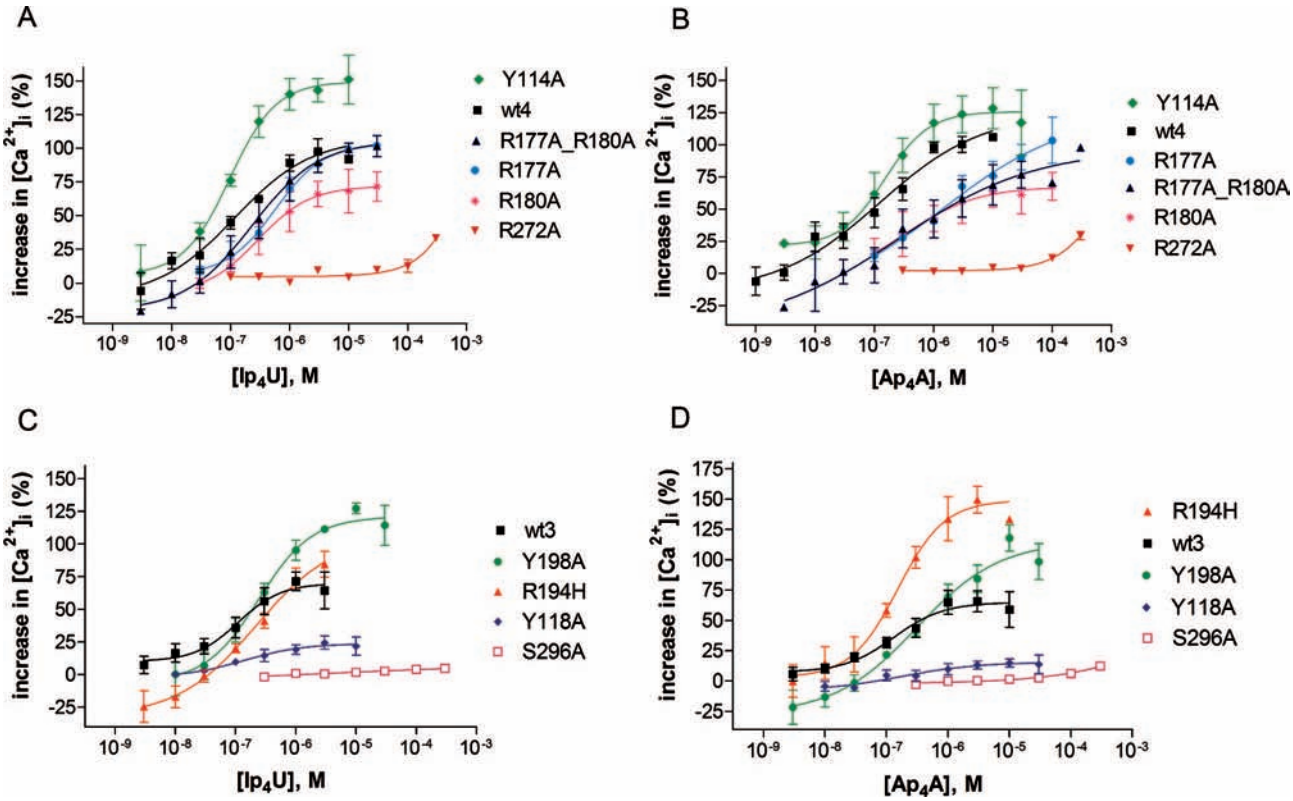


**Figure 7.** Dinucleotide activation of P2Y$_2$R mutants ($n = 3-6$). (A) Ip$_4$U activation of highly expressed mutants. (B) Ap$_4$A: activation of highly expressed mutants. (C) Ip$_4$U activation of mutants with intermediate expression rates. (D) Ap$_4$A: activation of mutants with intermediate expression rates.

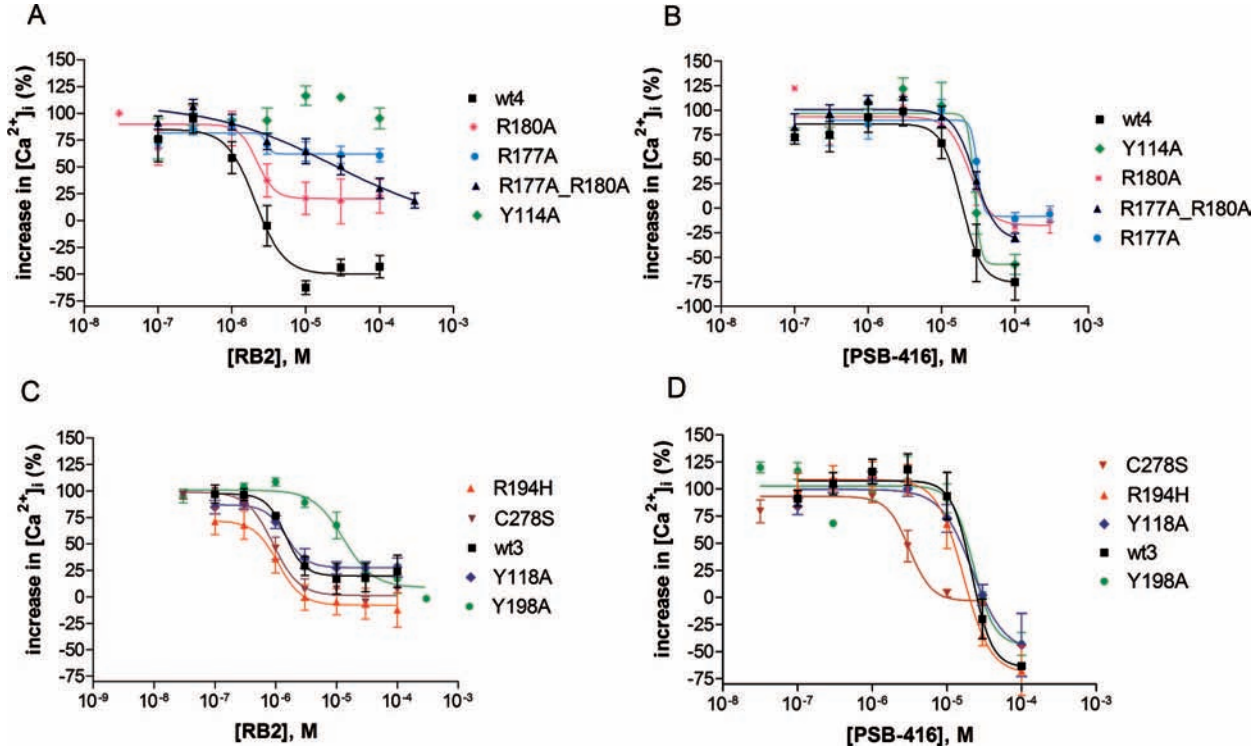


**Figure 8.** Inhibition of UTP-induced calcium mobilization at P2Y$_2$ receptor wild-type and mutants stably expressed in 1321N1 astrocytoma cells. 1321N1 cells expressing the wild-type or a mutated P2Y$_2$R were preincubated with antagonist for 20 min. $[Ca^{2+}]_i$ was determined for a range of antagonist concentrations after UTP stimulation ($n = 3-6$). (A,B) Effects of the inhibitor RB2 (**6**). (C,D) Effects of the inhibitor PSB-416 (**8**). For IC$_{50}$ values, see Table 3.

valuable information for the development of novel agonists and antagonists. Furthermore, it would contribute to the understanding of the structure and function of GPCRs in general and P2Y and P2Y-like receptors in particular, especially because the P2Y$_2$ receptor subtype is highly promiscuous toward a variety of nucleotides being activated

**Table 3.** Inhibitory Effects of Antagonists on UTP-Induced Calcium Mobilization in Wild Type and Mutant $P2Y_2$ Receptors[a]

| mutant | RB2 (**6**) $IC_{50} \pm$ SEM ($\mu$M) | PSB-416 (**8**) $IC_{50} \pm$ SEM ($\mu$M) |
|---|---|---|
| wt4 | $1.85 \pm 0.39$ | $21.7 \pm 5.2$ |
| Y114A | **≫100** | $24.6 \pm 3.9$ |
| R177A_R180A | **$18.6 \pm 6.2$*[c]** | $26.5 \pm 3.3$ |
| R177A | $3.36 \pm 1.24$[b] | $30.8 \pm 0.7$ |
| R180A | $2.1 \pm 0.34$[b] | $23.4 \pm 3.5$ |
| R272A | nd | nd |
| wt3 | $1.62 \pm 0.27$ | $21.9 \pm 3.9$ |
| Y118A | $1.57 \pm 0.29$ | $22.4 \pm 6.3$ |
| R194H | $1.00 \pm 0.23$ | $17.6 \pm 3.7$ |
| Y198A | **$9.30 \pm 2.28$*[c]** | $21.1 \pm 2.9$ |
| S296A | nd | nd |

[a] Concentration−inhibition curves for **6** and **8** were determined. Cells were stimulated with UTP at a concentration, leading to 80−90% of the maximal response, ($n = 3-6$). [b] no complete inhibition was observed (max. inhibition was ca. 55%). [c] *: $p < 0.05$ ($t$ test).

by adenine as well as uracil nucleotides and even by large, dimeric nucleotides such as diadenosine and diuridine tetraphosphate.

To achieve our goal, we combined homology modeling of the $P2Y_2$ receptor, docking of structurally diverse ligands including agonists and antagonists, mutagenesis studies of potentially relevant amino acids, and functional assays measuring intracellular calcium mobilization of the $G_q$-coupled $P2Y_2$ receptor. Additional radioligand binding studies would have been useful but could not be performed because a subtype-selective, high affinity radioligand for $P2Y_2$ receptors has not been developed to date.

HA-tagged wild type and mutant $P2Y_2R$ were stably expressed in 1321N1 astrocytoma cells, and receptor expression was quantified by ELISA. Cell lines with different receptor expression levels of the wild-type receptor were obtained, allowing a meaningful comparison of determined $EC_{50}$ values for expressed mutant receptors and a corresponding wild-type cell line of the same relative receptor expression level. This was useful to improve the accuracy of the results because $EC_{50}$ values typically depend on receptor expression levels.[55,59]

Receptor modeling was performed based on analogy to the crystal structure of bovine rhodopsin.[49] Recently, the crystal structure of a second GPCR, the $\beta_2$ adrenergic receptor, has been published,[50,51] but the $P2Y_2R$ sequence is slightly more homologous to that of bovine rhodopsin. The transmembrane regions of the $\beta_2$ adrenergic receptor are in very good accordance with those of rhodopsin as well as the generated model (Supporting Information Figure 5E). This finding confirms that homology models based on bovine rhodopsin are suitable for studying class A GPCRs.[52] The location of the binding sites for UTP and ATP in our model was roughly in accordance with a previously published model.[19,39] Furthermore, our model showed that the entry channel to the binding site was located between TM5 and TM6. Very recently, a crystal structure of the ligand-free bovine rhodopsin, presumably constituting an active conformation of rhodopsin, was published, proposing a very similar uptake route for retinal between TM5 and TM6, indicating that this is probably a general mechanism.[60] Molecular dynamics simulation studies of the receptor model embedded into a phospholipid bilayer and surrounded by water molecules and sodium and chloride ions showed subtle differences for UTP, ATP, and $Ap_4A$: UTP and ATP show a slightly shifted binding mode and therefore interact somewhat differently with the amino acid residues in the binding pocket (Figures 9B,C,E and Supporting Information Figures 1 and 2). These differences were confirmed by mutagenesis studies because exchange of amino acids had in many cases quantitatively different effects on ATP vs UTP activity. Furthermore, the binding pocket for UTP is smaller due to a larger induced fit of the receptor protein (Figure 9E). As a consequence, the interaction energy for the UTP receptor complex is higher than that for the ATP complex, and consistent with this, UTP is a slightly more potent and more efficacious agonist than ATP (Table 1, 2). On the other hand, for the large dinucleotide $Ap_4A$, a lower degree of induced fit by the protein is observed, and the ligand has to adapt its conformation in order to fit into the binding site. Although the dinucleotides (being large molecules) can have more interactions with the receptor protein than the mononucleotides, their potency is lower. This may be explained by their suboptimal fit into the receptor binding site. As seen in Figure 9F, part of the dinucleotide $Ap_4A$ sticks out of the receptor protein. Dinucleotide binding would result in reduced flexibility of the receptor protein, including EL2, which is part of the binding pocket for mononucleotides. This may explain the reduced efficacy of the dinucleotides investigated (Table 2) as observed in our test system. Christopoulos and colleagues have recently shown that a flexible EL2 is required for activation of the $M_2$ muscarinic receptor, another prototypical class A GPCR.[61]

R272 at the beginning of EL3 close to the end of TM6 appears to be the gatekeeper: the basic amino acid may initially interact with the negatively charged ligands and guide them down to their final destination. In addition, it also serves as part of an extended binding pocket for larger ligands such as the dinucleotide $Ap_4A$ (Supporting Information Figure 3). Mutation of this amino acid had dramatic consequences: the receptor still could be activated, albeit with reduced maximal effect, but the agonist curves were shifted to the right by several-hundred-fold and even more for dinucleotides ($Ap_4A$, $Ip_4U$) than for mononucleotides (ATP, UTP) (Figures 6 and 7 and Table 2). The presence of a basic amino acid at the beginning of EL3 is highly conserved among related GPCRs such as other P2Y receptor subtypes, GPR17, cysteinyl leukotriene receptors, and prostaglandin D2 receptors (see Supporting Information Figure 6), all of which are activated by negatively charged agonists. This suggests a general role either in initial recognition or in ligand binding of anionic ligands at GPCRs.

The surrounding of the entrance channel leading to the ligand binding site is lined with aromatic amino acids, in particular phenylalanine and tyrosine residues (Figure 9G). These amino acids facilitate the sliding of the ligands into the ligand binding pocket. After initial contact, the nucleotides most likely enter the channel with their lipophilic site (the uracil or adenine moiety) ahead, gliding down the aromatically lined upper part of the channel to reach the final site. The pocket also contains several serine and threonine residues, which can form hydrogen bonds with the ribose moiety, and the three positively charged amino acids H262 (6.52), R265 (6.55), and R292 (7.39), which are required for binding and orientation of the phosphate chain. These three basic amino acids have already been shown in a previous mutagenesis study to be involved in nucleotide binding to the $P2Y_2R$.[28]

For the first time, antagonists have been docked into a $P2Y_2R$ model. The antagonist **6**, a relatively large molecule, and the smaller **8**, can bind to the same binding site as agonists. However, different amino acids interact with the antagonist molecules and therefore the effects of mutagenesis on antagonist potencies are very different from the effects on agonists potencies and efficacies. Compound **6**, a rather large molecule with three negatively charged sulfonate moieties, exhibited an extremely high interaction energy when docked into the binding

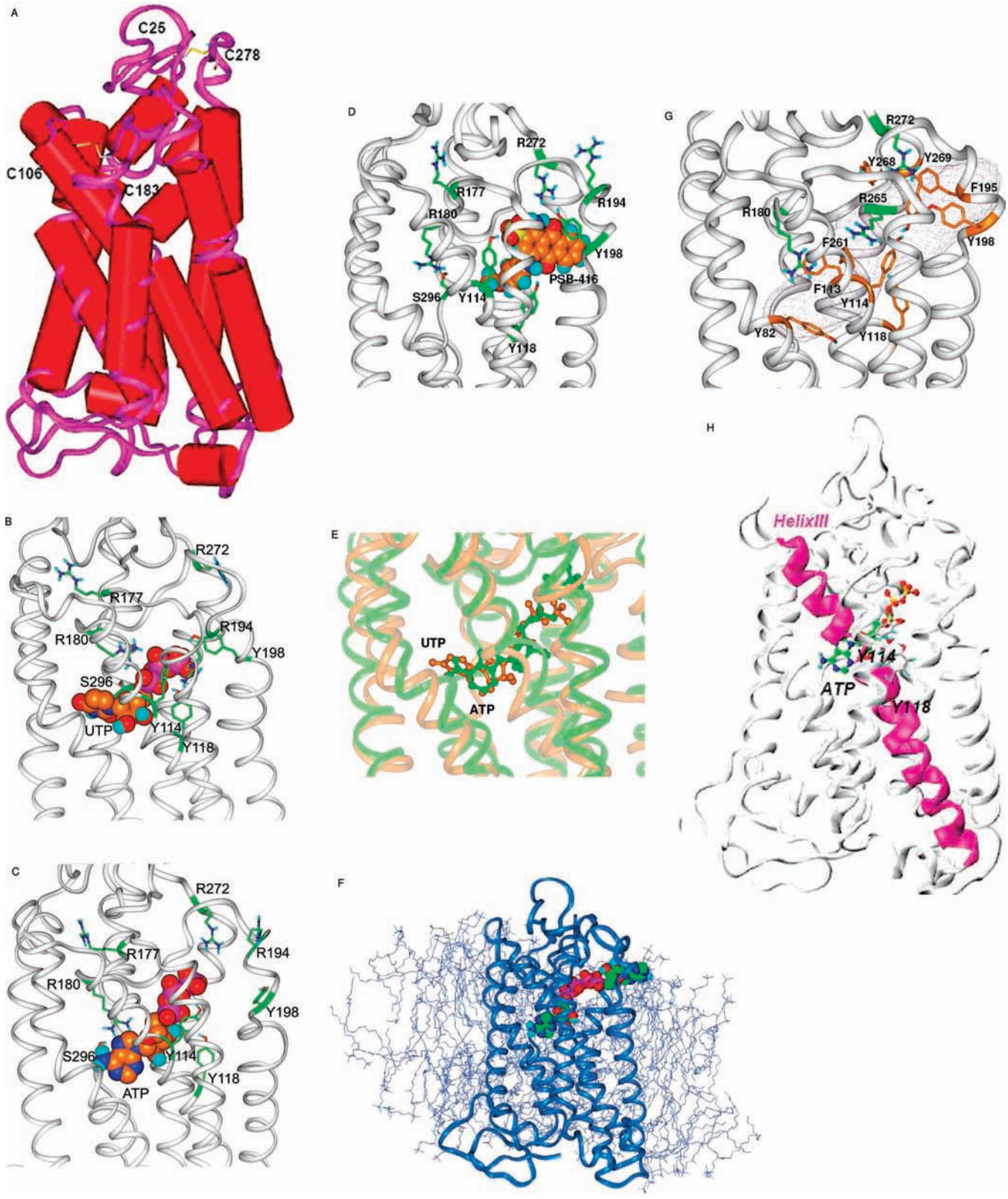


**Figure 9.** Computer-generated model of the human P2Y$_2$ receptor. (A) Three-dimensional model of the P2Y$_2$R and its disulfide bridges. (B,C,D) Binding sites of ATP, UTP, and PSB-416 (**8**) in the upper part of the transmembrane helices of the receptor are shown. (E) Comparison of ATP (green) and UTP (brown) binding modes in the P2Y$_2$ receptor as well as helix orientation in the bound conformation. (F) P2Y$_2$ receptor embedded in a lipid bilayer with Ap$_4$A docked into the binding site. (G) Position of the entry channel within the transmembrane helices. (H) Amino acids Y114 (3.33) and Y118 (3.36) are positioned in the binding pocket of the P2Y$_2$R. Y118 interacts with nucleotide agonists, while Y114 shows strong interaction with the antagonist RB2 (**6**) (not shown).

pocket; nevertheless, IC$_{50}$ values were comparatively high (1.85 $\mu$M). This discrepancy may be explained by the fact that the negatively charged sulfonate groups of **6**, which are not adjacent as in the nucleotides but distributed all over the molecule, could interact with amino acids in the outer parts of the receptor protein. Compound **6** may therefore exhibit many different

binding modes and cover the entry channel rather than diving down into the agonist site. In contrast, the small molecule **8**, which has only a single sulfonate group, will most likely bind inside the receptor protein (Figure 9D, Supporting Information Figure 4). The lipophilic methoxyl substituent of the aniline moiety enters the channel and is expected to bind deep down in the vicinity of the nucleobase site, while the negatively charged anthraquinone residue will bind toward the upper part of the receptor protein (in analogy to the binding mode of ATP and UTP). The model shows that there are regions that are not occupied by the small antagonist and will therefore allow for ligand optimization.

The obtained mutational data are well in accordance with and support the computer-generated receptor model. According to our theoretical and experimental data, EL2 dips deep into the binding pocket of the $P2Y_2R$ and R180 directly interacts with the nucleobase moiety (adenine or uracil) of the agonists (see Supporting Information). It had previously been reported that EL2 plays an important role in ligand binding and receptor activation of many class A GPCRs.[29,30,61−65] According to our receptor model, the interaction of R180 with ATP is tighter than with UTP, and this is also reflected in the larger increase in $EC_{50}$ values for ATP than for UTP in the R180A mutant (4-fold vs 2-fold). While the double mutant R180A_R177A behaved very similarly to the R180A mutant, the R177A mutant showed somewhat increased $EC_{50}$ values, particularly for the adenine nucleotides ATP and $Ap_4A$ but not for UTP. R177 (EL2) is located near R180, but its side chain is too distant from the ligands to allow direct interactions (Supporting Information Figure 5A,B). R177 points toward the outside of the receptor and appears to play a role in stabilizing the receptor conformation. In contrast to our findings, a model based on a lower number of mutagenesis data suggested that the basic amino acids in EL2, R177, R180, and R194 form electrostatic bridges with negatively charged residues in the N-terminus or the EL2.[19]

Mutation of Y118 (3.37) to alanine in TM3 led to a dramatic reduction in the efficacy of all agonists. According to our model, Y118 (3.37) is part of the ligand entry channel and at the same time part of the triphosphate binding site (Figure 9H). It may propagate effects by the formation of aromatic clusters with other aromatic amino acids near the binding pocket. In contrast, mutation of Y114 (3.33) to alanine in TM3 had only minor effects on agonist potencies and efficacies (it slightly increased the potency of ATP (2-fold) and the efficacy of $Ip_4U$ (from 98% at the wild-type to 142%). However, it completely abolished binding of the antagonist **6** (Table 3), showing that the interaction partners for agonists and antagonists can be very different. A similar effect was seen with the Y198A mutant (top of TM5 near the entrance site). It led to somewhat increased efficacies for all agonists investigated, indicating that it has an effect on receptor conformation and led to a 5-fold reduction in the antagonistic potency of **6**.

Compound **6** showed decreased inhibitory efficacy at the arginine mutants R177A_R180A, R177A, and R180A in EL2. Remarkably, the antagonist could only partly inhibit UTP-induced calcium mobilization, even at high concentrations of the antagonist. This may be a further indication that **6** actually exhibits different binding modes. Removal of the basic amino acids in EL2, which is part of the binding pocket, may shift the equilibrium toward extracellular, noncompetitive binding of **6**. This may then modulate receptor activation.

Interestingly, the mutant R194H in EL2 induced a large, significant increase in efficacy of the agonists UTP, ATP, and $Ap_4A$, while $EC_{50}$ values were unaltered. Together with R272 (EL3), which has strong effects on agonist potencies, R194 is located at the entry channel into the receptor protein. These basic residues appear to be responsible for the first contact of the ligand with the $P2Y_2R$ and seem to position it adequately for entry into the binding pocket. A homologous exchange of R194 for histidine was even more favorable for receptor activation probably due to steric effects. Interestingly, R194 is replaced by His in other species including mouse, rat, and boar, suggesting that in those animals $P2Y_2$ agonists may be more efficacious or more potent than in humans.

S296 (7.43) was found to be an essential amino acid absolutely required for receptor activation (Supporting Information Figure 5D). It is localized in TM7 deep down in the binding pocket, where it can interact with the nucleobase moieties of the agonists via a water molecule. In addition, it is crucial for the stability of TM7 by forming a stable hydrogen bond with P293 (7.40). Our experimental data confirm the model by Ivanov et al., who postulated a similar role for S296 in their receptor model.[19] Mutation of the homologous S314 (7.43) in the $P2Y_1$ receptor also resulted in an inactive receptor.[29]

The $P2Y_2$ receptor forms two disulfide bridges, i.e., between C25−C278 and C106−C183, both of which are essential for receptor function. These cysteine residues are highly conserved among other P2Y receptor subtypes, where they are predicted to form comparable disulfide bonds.[4,19,66,67] Chemical reduction of these disulfide bridges with DTT led to a large decrease in receptor activation but had only a moderate effect on activation of the M3 receptor. Our data suggest that the disulfide bridges of the M3 receptor are buried in the inner part of the receptor protein and are therefore not accessible to externally applied reducing agents. In contrast, at least one of the essential disulfide bridges in the $P2Y_2R$ is easily accessible by disulfide-reducing chemicals and therefore is expected to be exposed at the surface of the receptor protein. In the next step, one cysteine out of each disulfide bridge was mutated to serine (C106S, C278S). The mutant C106S could not be expressed in 1321N1 astrocytoma cells, suggesting that the disulfide bridge C106−C183 is essential for proper protein folding and integration in the cell membrane. This disulfide bridge is conserved in all GPCRs. The mutant C278S could be expressed and was subsequently monitored for activation by agonists. C278S exhibited increased $EC_{50}$ values for all tested agonists. Purine nucleotides were affected more strongly than pyrimidines, and for dinucleotides the effect was even stronger, inducing a rightward shift of more than 3 orders of magnitude. It appears likely that the disulfide bridge between C278 and C25 stabilizes and constrains the conformation of the receptor binding channel. The binding site may become larger and more flexible when the disulfide bridge is missing, which would explain the decrease in affinity. The disulfide bridge between the N-terminus and EL3 is typical for all P2Y receptor subtypes and was also shown to be critical for the $P2Y_1$ receptor.[33]

In contrast to the results obtained with agonists, effects on the potencies of the antagonists **6** and **8** were only moderate. C278S showed no change in **6** potency compared to the wild-type receptor; however, the $IC_{50}$ value of the small anthraquinone derivative **8** was actually decreased (3.44 $\mu$M vs 21.9 $\mu$M). One possibility to explain this result is that this compound can enter the binding pocket more easily due to the absence of the disulfide bridge.

The $P2Y_2$ receptor model previously published by Ivanov et al.[19] showed roughly the same binding orientation for UTP as the present model. However, our model is more detailed and

refined. The receptor was embedded in a virtual membrane environment, and molecular dynamics studies were conducted for the receptor−ligand complexes. We have discovered and rationalized a role for the basic amino acids R272 and R194 in the extracellular loops. Furthermore, we describe for the first time a lipophilic channel, which is part of the binding site for larger ligands, such as dinucleotides. Another major difference between the previous and the present model is that we propose a direct interaction of negatively charged residues in the EL2 with the nucleotide, while Ivanov and colleagues suggested electrostatic bridges between EL2 and amino acids in other parts of the receptor.

## Conclusions

In conclusion, we identified and confirmed amino acids in the binding pocket, of which EL2 is a part, that are important for receptor binding and/or activation. We provide a refined model of the $P2Y_2$ nucleotide receptor based on experimental data, which rationalizes the promiscuity of the receptor toward structurally diverse nucleotides and provides information on antagonist binding. The model will allow for the design of more potent $P2Y_2$ receptor antagonists, which are urgently required as pharmacological tools and have considerable potential as novel drugs. We propose a mechanism of initial receptor−ligand recognition, ligand orientation, and subsequent movement into the binding pocket. The current results may be of general importance not only for other P2Y receptor subtypes but for the important family of class A GPCR.

## Experimental Section

**Materials.** $Ip_4U$ (INS45973) was prepared at Inspire Pharmaceuticals Inc. (Durham, NC) as previously described by Shaver et al. with a purity of >98%.[40] Restriction enzymes and VentR DNA polymerase were purchased from New England Biolabs (Frankfurt, Germany), antibiotics, LB agar, and hygromycin B were obtained from Calbiochem (Darmstadt, Germany), Reactive Blue 2 (**6**), 2,2′-azino-bis-(3-ethylbenzthiazoline-6-sulfonic acid) (ABTS), and fetal calf serum (FCS) from Sigma-Aldrich (Taufkirchen, Germany), and Oregon Green BAPTA-1/AM from Invitrogen (Carlsbad, CA). Dulbecco's modified Eagle medium (DMEM), ultraglutamine, and trypsine were purchased from Cambrex (Taufkirchen, Germany). All other chemicals were purchased from AppliChem (Darmstadt, Germany) unless stated otherwise. Primers were synthesized by MWG Biotech (Ebersberg, Germany).

**Cell Culture.** 1321N1 astrocytoma cells were cultured at 37 °C, 96% humidity, and 5% $CO_2$ in DMEM supplemented with 10% FCS, 100 U/mL penicillin G, 100 $\mu$g/mL streptomycin, and 1% ultraglutamine. After stable transfection, penicillin and streptomycin were replaced by 800 $\mu$g/mL Geneticin (G418). GP+envAM12 packaging cells were maintained in HXM media containing DMEM supplemented with 10% FCS, 100 U/mL penicillin G, 100 $\mu$g/mL streptomycin, 1% ultraglutamine, 15 $\mu$g/mL hypoxanthine, 250 $\mu$g/mL xanthine, 25 $\mu$g/mL mycophenolic acid, and 200 $\mu$g/mL hygromycin B under the same conditions.

**Site-Directed Mutagenesis.** The human coding sequence for the $P2Y_2$ receptor was cloned into the retroviral expression vector pLXSN.[41] The influenza virus hemagglutinin (HA) epitope was added to the N-terminus of the receptor. It had been shown previously that the HA-tag does not alter the pharmacological properties of the $P2Y_2R$.[36] Point mutations were introduced into the plasmid using whole plasmid recombination PCR.[42] Primers are shown in Supporting Information Table 1. PCR was performed as follows: 3 min at 94 °C, 20 cycles consisting of 1 min at 94 °C, 1 min at appropriate annealing temperatures (Supplemental Data Table 1), and 13 min primer extension at 72 °C. This was followed by a final extension of 15 min at 72 °C. After digest with DpnI, the DNA was transformed into *Echerichia coli* and isolated from individual clones. Sequencing was performed by GATC Biotech (Konstanz, Germany).

**Retroviral Transfection of 1321N1 Astrocytoma Cells.** GP+envAM12 packaging cells[43] were plated at a density of $1.5 \times 10^6$ into 25 $cm^2$ flasks using DMEM containing 10% FCS, 100 U/mL penicillin G, 100 $\mu$g/mL streptomycin, and 1% ultraglutamine 24 h before transfection. The cells were transfected using lipofectamine 2000 (Invitrogen, Karlsruhe, Germany). To increase infection efficiency, receptor DNA (63%) was mixed with vesicular stomatitis virus G protein (VSV-G) DNA (37%)[44] prior to transfection. After 16 h, the medium was replaced by 3 mL of medium containing 5 mM sodium butyrate. The transfected GP+envAM12 cells were cultured at 32 °C, 96% humidity, and 5% $CO_2$ for 48 h. The supernatant of the GP+envAm12 cells was collected and mL of the virus solution was mixed with 4 $\mu$L of polybrene (4 mg/ml) and incubated for 2.5 h at 37 °C with 1321N1 astrocytoma cells. After 48 h, these cells were selected for Geneticin resistance in the presence of 800 $\mu$g/mL G418.

**Cell Surface ELISA.** 1321N1 astrocytoma cells stably expressing the P2Y2R or its mutants, were transferred to 24-well plates (Greiner Bio One, Frickenhausen, Germany) in duplicates at a density of 150000 cells per well 24 h before initiation of the assay ($n = 3-8$). Every step of the ELISA except for antibody incubation and substrate reaction was performed on ice using 500 $\mu$L of ice-cold buffers and solutions. Cell surfaces were blocked using 1% BSA dissolved in phosphate-buffered saline (PBS) containing 137 mM NaCl, 2.7 mM KCl, 4.3 mM $Na_2HPO_4$, and 1.47 mM $KH_2PO_4$, pH adjusted to 7.4. Cells were then incubated with 300 $\mu$L of a 1:1000 dilution of HA-specific monoclonal antibody solution (HA.11, Covance, Berkley, CA) in DMEM, 1% BSA, 10 $\mu$M HEPES, pH 7.0, and 1 $\mu$M $CaCl_2$ for 1 h at room temperature. After washing, cells were fixed with 4% paraformaldehyde for 5 min and washed again. 1321N1 astrocytoma cells were blocked for 10 min with 1% BSA and then incubated with peroxidase-conjugated goat antimouse IgG antibody (1:2500) (Sigma-Aldrich, Taufkirchen, Germany). Cells were washed repeatedly with PBS and covered with 300 $\mu$L of ABTS solution for 45 min at room temperature. Then 170 $\mu$L aliquots of the substrate were transferred to a 96-well plate and absorbance was determined at 405 nm using a FLUOstar plate reader (BMG Laboratory Technologies, Offenburg, Germany).

**Chemical Reduction of Disulfide Bridges.** To investigate the role of potential disulfide bridges for $P2Y_2$ receptor activation, 1321N1 cells expressing the wild-type receptor were preincubated with dithiothreitol (DTT, 1 mM or 10 mM) as described previously for angiotensin II receptors.[45] After 15 min, the cells were stimulated with UTP or ATP, respectively, and intracellular $Ca^{2+}$ levels were measured.

**Determination of Intracellular $Ca^{2+}$ Concentrations.** $Ca^{2+}$ measurements were performed as described previously using a NOVOstar plate reader (BMG LabTechnologies, Offenburg, Germany).[46−48] Cells from two 175 $cm^2$ flasks were transferred to a 50 mL tube and kept at 37 °C, 96% humidity, 5% $CO_2$ for 30 min. After centrifugation (200*g*, 4 °C, 5 min) cells were resuspended in Krebs−HEPES buffer containing NaCl 118.6 mM, KCl 4.7 mM, $KH_2PO_4$ 1.2 mM, $NaHCO_3$ 4.2 mM, D-glucose 11.7 mM, HEPES (free acid) 10 mM, $CaCl_2$ 1.3 mM, and $MgSO_4$ 1.2 mM. The pH of the buffer was adjusted to 7.4 using NaOH. The cells were incubated in a final volume of 1 mL at room temperature (continuous spinning for 1 h at 10 rpm, exclusion of light) with 3 $\mu$L of a 1 mM solution of Oregon Green BAPTA-1/AM, which had been mixed with a 20% solution of Pluronic F-127 in DMSO at a ratio 1:1 immediately before use. Then cells were rinsed twice with Krebs−HEPES buffer, diluted, and plated into a 96-well plate (black, uclear, Greiner Bio-One, Frickenhausen, Germany) at a density of 150000 cells per well in a volume of 180 $\mu$L. For testing of antagonists, 20 $\mu$L of a 10-fold concentrated test compound solution was added to 160 $\mu$L of the cell suspension prior to the measurement. For receptor stimulation in the presence of antagonists, UTP was added in a concentration that led to 80−90% of maximal response to receptor activation. The plates were kept at

28 °C under exclusion of light for 20 min until the measurement was started. Agonist solution in buffer (20 $\mu$L) was injected sequentially into separate wells and fluorescence was measured at 520 nm (bandwidth 25 nm) for 60 intervals of 0.4 s each. The excitation wavelength was 485 nm.

**Data Analysis.** Concentration−response curves were generated by plotting mean values of average fluorescence intensity change using nonlinear regression with a sigmoidal dose−response equation (Prism 3.0, GraphPad Software, San Diego, CA) as previously described.[47] To determine *p* values, unpaired *t* tests with 95% confidence intervals were used.

**Homology Modeling.** The crystal structure (2.2 Å) of bovine rhodopsin (PDB 1U19) was used as a template, i.e., the helix backbone coordinates of the crystal structure were adopted as far as possible.[49] Comparison with the recently published X-ray structure of the $\beta$2-adrenergic receptor[50,51] showed a very good agreement of both structures.[52,53] All loop regions were generated by applying the homology modeling module of the program INSIGHT. SCWRL 3.0 was applied to select the energetically most favorable side chain conformations. To refine and examine the protein structure, several molecular dynamics (MD) simulations were carried out. For this purpose, the receptor model was embedded into a dipalmitoylphosphatidylcholine (DPPC) lipid bilayer surrounded above and below by water containing $Cl^-$ and $Na^+$ ions to mimic physiological conditions. Agonists were docked into a relaxed protein structure with SURFLEX-DOCK. Antagonists were docked into a relaxed representative protein structure of the $Ap_4A$ MD simulation. The applied procedures have been described by Ko in detail.[53]

**Acknowledgment.** We are very grateful to Dr. José Boyer, Inspire Pharmaceuticals, Inc., Durham, NC, for the gift of $Ip_4U$ (INS45973), and to Dr. Younis Baqi and Dr. Stefanie Weyler for the synthesis and purification of antagonists. Dr. Volkmar Gieselmann is acknowledged for providing GP+envAM12 cells and Dr. Anke C. Schiedel for helpful discussion. We thank Dr. T. Kendall Harden, Dr. JoAnn Trejo, and Breann L. Wolfe for support and advice. This study was funded by the Deutsche Forschungsgemeinschaft (Graduiertenkolleg GRK804 and GRK677).

**Supporting Information Available:** Primer sequences, additional information on $P2Y_2$ receptor model and ligand docking, and alignments of the extracellular loop 3 of nucleotide receptors. This material is available free of charge via the Internet at http://pubs.acs.org.



## References

(1) Lagerström, M. C.; Rabe, N.; Haitina, T.; Kalnina, I.; Hellström, A. R.; Klovins, J.; Kullander, K.; Schiöth, H. B. The evolutionary history and tissue mapping of GPR123: specific CNS expression pattern predominantly in thalamic nuclei and regions containing large pyramidal cells. *J. Neurochem.* **2007**, *100*, 1129–1142.
(2) Lagerström, M. C.; Schiöth, H. B. Structural diversity of G protein-coupled receptors and significance for drug discovery. *Nat. Rev. Drug Discovery* **2008**, *7*, 339–357.
(3) Abbracchio, M. P.; Burnstock, G.; Boeynaems, J.-M.; Barnard, E. A.; Boyer, J. L.; Kennedy, C.; Knight, G. E.; Fumagalli, M.; Gachet, C.; Jacobson, K. A.; Weisman, G. A. International Union of Pharmacology. LVIII. Update on the P2Y G protein-coupled nucleotide receptors: from molecular mechanisms and pathophysiology to therapy. *Pharmacol. Rev.* **2006**, *58*, 281–341.
(4) Moro, S.; Hoffmann, C.; Jacobson, K. A. Role of the extracellular loops of G protein-coupled receptors in ligand recognition: a molecular modeling study of the human P2Y1 receptor. *Biochemistry* **1999**, *38*, 3498–3507.
(5) Bobbert, P.; Schlüter, H.; Schultheiss, H. P.; Reusch, H. P. Diadenosine polyphosphates Ap3A and Ap4A, but not Ap5A or Ap6A, induce proliferation of vascular smooth muscle cells. *Biochem. Pharmacol.* **2008**, *75*, 1966–1973.
(6) Burnstock, G. Purine and pyrimidine receptors. *Cell. Mol. Life Sci.* **2007**, *64*, 1471–1483.
(7) Burnstock, G. Purinergic signalling. *Br. J. Pharmacol.* **2006**, *147*, 172–181.
(8) Guns, P. J.; Van Assche, T.; Fransen, P.; Robaye, B.; Boeynaems, J. M.; Bult, H. Endothelium-dependent relaxation evoked by ATP and UTP in the aorta of P2Y2-deficient mice. *Br. J. Pharmacol.* **2006**, *147*, 569–574.
(9) Cressman, V. L.; Lazarowski, E.; Homolya, L.; Boucher, R. C.; Koller, B. H.; Grubb, B. R. Effect of loss of $P2Y_2$ receptor gene expression on nucleotide regulation of murine epithelial $Cl^-$ transport. *J. Biol. Chem.* **1999**, *274*, 26461–26468.
(10) Weisman, G. A.; Wang, M.; Kong, Q.; Chorna, N. E.; Neary, J. T.; Sun, G. Y.; Gonzalez, F. A.; Seye, C. I.; Erb, L. Molecular determinants of P2Y2 nucleotide receptor function: implications for proliferative and inflammatory pathways in astrocytes. *Mol. Neurobiol.* **2005**, *31*, 169–183.
(11) Franke, H.; Krügel, U.; Illes, P. P2 receptors and neuronal injury. *Pflügers Arch.* **2006**, *452*, 622–644.
(12) Pines, A.; Bivi, N.; Vascotto, C.; Romanello, M.; D'Ambrosio, C.; Scaloni, A.; Damante, G.; Morisi, R.; Filetti, S.; Ferretti, E.; Quadrifoglio, F.; Tell, G. Nucleotide receptors stimulation by extracellular ATP controls Hsp90 expression through APE1/Ref-1 in thyroid cancer cells: a novel tumorigenic pathway. *J. Cell. Physiol.* **2006**, *209*, 44–55.
(13) Coutinho-Silva, R.; Stahl, L.; Cheung, K. K.; de Campos, N. E.; de Oliveira Souza, C.; Ojcius, D. M.; Burnstock, G. P2X and P2Y purinergic receptors on human intestinal epithelial carcinoma cells: effects of extracellular nucleotides on apoptosis and cell proliferation. *Am. J. Physiol. Gastrointest. Liver Physiol.* **2005**, *288*, G1024–1035.
(14) Deterding, R.; Retsch-Bogart, G.; Milgram, L.; Gibson, R.; Daines, C.; Zeitlin, P. L.; Milla, C.; Marshall, B.; Lavange, L.; Engels, J.; Mathews, D.; Gorden, J.; Schaberg, A.; Williams, J.; Ramsey, B. Safety and tolerability of denufosol tetrasodium inhalation solution, a novel P2Y2 receptor agonist: results of a phase 1/phase 2 multicenter study in mild to moderate cystic fibrosis. *Pediatr. Pulmonol.* **2005**, *39*, 339–348.
(15) Nichols, K. K.; Yerxa, B.; Kellerman, D. J. Diquafosol tetrasodium: a novel dry eye therapy. *Expert Opin. Investig. Drugs* **2004**, *13*, 47–54.
(16) Vollmayer, P.; Clair, T.; Goding, J. W.; Sano, K.; Servos, J.; Zimmermann, H. Hydrolysis of diadenosine polyphosphates by nucleotide pyrophosphatases/phosphodiesterases. *Eur. J. Biochem.* **2003**, *270*, 2971–2978.
(17) Brunschweiger, A.; Müller, C. E. P2 receptors activated by uracil nucleotides−an update. *Curr. Med. Chem.* **2006**, *13*, 289–312.
(18) El-Tayeb, A.; Qi, A.; Müller, C. E. Synthesis and structure−activity relationships of uracil nucleotide derivatives and analogues as agonists at human P2Y2, P2Y4, and P2Y6 receptors. *J. Med. Chem.* **2006**, *49*, 7076–7087.
(19) Ivanov, A. A.; Ko, H.; Cosyn, L.; Maddileti, S.; Besada, P.; Fricks, I.; Costanzi, S.; Harden, T. K.; Calenbergh, S. V.; Jacobson, K. A. Molecular modeling of the human P2Y2 receptor and design of a selective agonist, 2′-amino-2′-deoxy-2-thiouridine 5′-triphosphate. *J. Med. Chem.* **2007**, *50*, 1166–1176.
(20) Nahum, V.; Tulapurkar, M.; Levesque, S. A.; Sevigny, J.; Reiser, G.; Fischer, B. Diadenosine and diuridine poly(borano)phosphate analogues: synthesis, chemical and enzymatic stability, and activity at P2Y1 and P2Y2 receptors. *J. Med. Chem.* **2006**, *49*, 1980–1990.
(21) Tulapurkar, M. E.; Laubinger, W.; Nahum, V.; Fischer, B.; Reiser, G. Subtype specific internalization of $P2Y_1$ and $P2Y_2$ receptors induced by novel adenosine 5′-*O*-(1-boranotriphosphate) derivatives. *Br. J. Pharmacol.* **2004**, *142*, 869–878.
(22) Pendergast, W.; Siddiqi, S. M.; Rideout, J. L.; James, M. K.; Dougherty, R.W. Stabilized uridine triphosphate analogs as agonists of the P2Y2 purinergic receptor. *Drug Dev. Res.* **1996**, *37*, Abstract 133.
(23) Pendergast, W.; Yerxa, B. R.; Douglass, J. G., III; Shaver, S. R.; Dougherty, R. W.; Redick, C. C.; Sims, I. F.; Rideout, J. L. Synthesis and P2Y receptor activity of a series of uridine dinucleoside 5′-polyphosphates. *Bioorg. Med. Chem. Lett.* **2001**, *11*, 157–160.
(24) Brown, J.; Brown, C. A. Evaluation of reactive blue 2 derivatives as selective antagonists for P2Y receptors. *Vasc. Pharmacol.* **2002**, *39*, 309–315.
(25) Charlton, S. J.; Brown, C. A.; Weisman, G. A.; Turner, J. T.; Erb, L.; Boarder, M. R. PPADS and suramin as antagonists at cloned P2Y- and P2U-purinoceptors. *Br. J. Pharmacol.* **1996**, *118*, 704–710.
(26) (a) Weyler, S.; Baqi, Y.; Hillmann, P.; Kaulich, M.; Hunder, A. M.; Müller, I. A.; Müller, C. E. Combinatorial synthesis of anilinoanthraquinone derivatives and evaluation as non-nucleotide-derived $P2Y_2$ receptor antagonists. *Bioorg. Med. Chem. Lett.* **2008**, *18*, 223–227. (b) Baqi, Y.; Müller, C. E. Rapid and efficient microwave-assisted copper(0)-catalyzed Ullmann coupling reaction: general access to anilinoanthraquinone derivatives. *Org. Lett.* **2007**, *9*, 1271–1274.
(27) Ballesteros, J. A.; Weinstein, H.; Stuart, C. S. Integrated methods for the construction of three-dimensional models and computational probing of structure-function relations in G protein-coupled receptors. In *Methods in Neurosciences*: Academic Press: New York, 1995.

(28) Erb, L.; Garrad, R.; Wang, Y.; Quinn, T.; Turner, J. T.; Weisman, G. A. Site-directed mutagenesis of P2U purinoceptors. Positively charged amino acids in transmembrane helices 6 and 7 affect agonist potency and specificity. *J. Biol. Chem.* **1995**, *270*, 4185–4188.
(29) Jiang, Q.; Guo, D.; Lee, B. X.; Van Rhee, A. M.; Kim, Y. C.; Nicholas, R. A.; Schachter, J. B.; Harden, T. K.; Jacobson, K. A. A mutational analysis of residues essential for ligand recognition at the human P2Y1 receptor. *Mol. Pharmacol.* **1997**, *52*, 499–507.
(30) Zylberg, J.; Ecke, D.; Fischer, B.; Reiser, G. Structure and ligand-binding site characteristics of the human P2Y11 nucleotide receptor deduced from computational modelling and mutational analysis. *Biochem. J.* **2007**, *405*, 277–286.
(31) Major, D. T.; Fischer, B. Molecular recognition in purinergic receptors. 1. A comprehensive computational study of the h-P2Y1-receptor. *J. Med. Chem.* **2004**, *47*, 4391–4404.
(32) Herold, C. L.; Qi, A. D.; Harden, T. K.; Nicholas, R. A. Agonist versus antagonist action of ATP at the P2Y4 receptor is determined by the second extracellular loop. *J. Biol. Chem.* **2004**, *279*, 11456–11464.
(33) Hoffmann, C.; Moro, S.; Nicholas, R. A.; Harden, T. K.; Jacobson, K. A. The role of amino acids in extracellular loops of the human P2Y1 receptor in surface expression and activation processes. *J. Biol. Chem.* **1999**, *274*, 14639–14647.
(34) Bagchi, S.; Liao, Z.; Gonzalez, F. A.; Chorna, N. E.; Seye, C. I.; Weisman, G. A.; Erb, L. The P2Y2 nucleotide receptor interacts with alphav integrins to activate Go and induce cell migration. *J. Biol. Chem.* **2005**, *280*, 39050–39057.
(35) Qi, A. D.; Wolff, S. C.; Nicholas, R. A. The apical targeting signal of the P2Y2 receptor is located in its first extracellular loop. *J. Biol. Chem.* **2005**, *280*, 29169–29175.
(36) Sromek, S. M.; Harden, T. K. Agonist-induced internalization of the P2Y2 receptor. *Mol. Pharmacol.* **1998**, *54*, 485–494.
(37) Garrad, R. C.; Otero, M. A.; Erb, L.; Theiss, P. M.; Clarke, L. L.; Gonzalez, F. A.; Turner, J. T.; Weisman, G. A. Structural basis of agonist-induced desensitization and sequestration of the P2Y2 nucleotide receptor. Consequences of truncation of the C terminus. *J. Biol. Chem.* **1998**, *273*, 29437–29444.
(38) Flores, R. V.; Hernandez-Perez, M. G.; Aquino, E.; Garrad, R. C.; Weisman, G. A.; Gonzalez, F. A. Agonist-induced phosphorylation and desensitization of the P2Y2 nucleotide receptor. *Mol. Cell. Biochem.* **2005**, *280*, 35–45.
(39) Jacobson, K. A.; Costanzi, S.; Ivanov, A. A.; Tchilibon, S.; Besada, P.; Gao, Z. G.; Maddileti, S.; Harden, T. K. Structure−activity and molecular modeling analyses of ribose- and base-modified uridine 5′-triphosphate analogues at the human P2Y2 and P2Y4 receptors. *Biochem. Pharmacol.* **2006**, *71*, 540–549.
(40) Shaver, S. R.; Rideout, J. L.; Pendergast, W.; Douglass, J. G.; Brown, E. G.; Boyer, J. L.; Patel, R. I.; Redick, C. C.; Jones, A. C.; Picher, M.; Yerxa, B. R. Structure−activity relationships of dinucleotides: Potent and selective agonists of P2Y receptors. *Purinergic Signalling* **2005**, *1*, 183–191.
(41) Miller, A. D.; Rosman, G. J. Improved retroviral vectors for gene transfer and expression. *Biotechniques* **1989**, *7*, 980–982; 984−986; 989−990.
(42) Reikofski, J.; Tao, B. Y. Polymerase chain reaction (PCR) techniques for site-directed mutagenesis. *Biotechnol. Adv.* **1992**, *10*, 535–547.
(43) Markowitz, D.; Goff, S.; Bank, A. A safe packaging line for gene transfer: separating viral genes on two different plasmids. *J. Virol.* **1988**, *62*, 1120–1124.
(44) Emi, N.; Friedmann, T.; Yee, J. K. Pseudotype formation of murine leukemia virus with the G protein of vesicular stomatitis virus. *J. Virol.* **1991**, *65*, 1202–1207.
(45) Heerding, J. N.; Hines, J.; Fluharty, S. J.; Yee, D. K. Identification and function of disulfide bridges in the extracellular domains of the angiotensin II type 2 receptor. *Biochemistry* **2001**, *40*, 8369–8377.
(46) Kassack, M. U.; Höfgen, B.; Lehmann, J.; Eckstein, N.; Quillan, J. M.; Sadee, W. Functional screening of G protein-coupled receptors by measuring intracellular calcium with a fluorescence microplate reader. *J. Biomol. Screen.* **2002**, *7*, 233–246.
(47) Kaulich, M.; Streicher, F.; Mayer, R.; Müller, I.; Müller, C. E. Flavonoids−novel lead compounds for the development of $P2Y_2$ receptor antagonists. *Drug Dev. Res.* **2003**, *59*, 72–81.
(48) Hillmann, P.; Köse, M.; Söhl, K.; Müller, C. E. Ammonium-induced calcium mobilization in 1321N1 astrocytoma cells. *Toxicol. Appl. Pharmacol.* **2008**, *227*, 36–47.
(49) Okada, T.; Sugihara, M.; Bondar, A. N.; Elstner, M.; Entel, P.; Buss, V. The retinal conformation and its environment in rhodopsin in light of a new 2.2 A crystal structure. *J. Mol. Biol.* **2004**, *342*, 571–583.
(50) Rasmussen, S. G.; Choi, H. J.; Rosenbaum, D. M.; Kobilka, T. S.; Thian, F. S.; Edwards, P. C.; Burghammer, M.; Ratnala, V. R.; Sanishvili, R.; Fischetti, R. F.; Schertler, G. F.; Weis, W. I.; Kobilka, B. K. Crystal structure of the human beta2 adrenergic G-protein-coupled receptor. *Nature (London)* **2007**, *450*, 383–387.
(51) Cherezov, V.; Rosenbaum, D. M.; Hanson, M. A.; Rasmussen, S. G.; Thian, F. S.; Kobilka, T. S.; Choi, H. J.; Kuhn, P.; Weis, W. I.; Kobilka, B. K.; Stevens, R. C. High-resolution crystal structure of an engineered human beta2-adrenergic G protein-coupled receptor. *Science* **2007**, *318*, 1258–1265.
(52) Costanzi, S. On the applicability of GPCR homology models to computer-aided drug discovery: a comparison between in silico and crystal structures of the beta2-adrenergic receptor. *J. Med. Chem.* **2008**, *51*, 2907–2914.
(53) Ko, G.-Y. Molecular Modelling Untersuchungen am humanen $P2Y_2$-Rezeptor und seinen Liganden (Molecular modelling studies at the human $P2Y_2$ receptor and its ligands). Ph.D. Thesis. Cuvillier: Düsseldorf, Germany, 2007 http://docserv.uni-duesseldorf.de/servlets/DerivateServlet/Derivate-7155/KO_pdfA.pdf.
(54) Kinzer-Ursem, T. L.; Linderman, J. J. Both ligand- and cell-specific parameters control ligand agonism in a kinetic model of g protein-coupled receptor signaling. *PLoS Comput. Biol.* **2007**, *3*, e6.
(55) Kenakin, T. Differences between natural and recombinant G protein-coupled receptor systems with varying receptor/G protein stoichiometry. *Trends Pharmacol. Sci.* **1997**, *18*, 456–464.
(56) Fonseca, M. I.; Lunt, G. G.; Aguilar, J. S. Inhibition of muscarinic cholinergic receptors by disulfide reducing agents and arsenicals. Differential effect on locust and rat. *Biochem. Pharmacol.* **1991**, *41*, 735–742.
(57) Arthur, D. B.; Akassoglou, K.; Insel, P. A. P2Y2 and TrkA receptors interact with Src family kinase for neuronal differentiation. *Biochem. Biophys. Res. Commun.* **2006**, *347*, 678–682.
(58) Seye, C. I.; Kong, Q.; Erb, L.; Garrad, R. C.; Krugh, B.; Wang, M.; Turner, J. T.; Sturek, M.; Gonzalez, F. A.; Weisman, G. A. Functional P2Y2 nucleotide receptors mediate uridine 5′-triphosphate-induced intimal hyperplasia in collared rabbit carotid arteries. *Circulation* **2002**, *106*, 2720–2726.
(59) Zhong, H.; Wade, S. M.; Woolf, P. J.; Linderman, J. J.; Traynor, J. R.; Neubig, R. R. A spatial focusing model for G protein signals. Regulator of G protein signaling (RGS) protein-mediated kinetic scaffolding. *J. Biol. Chem.* **2003**, *278*, 7278–7284.
(60) Park, J. H.; Scheerer, P.; Hofmann, K. P.; Choe, H. W.; Ernst, O. P. Crystal structure of opsin in its G-protein-interacting conformation. *Nature* **2008**, *454*, 183–187.
(61) Avlani, V. A.; Gregory, K. J.; Morton, C. J.; Parker, M. W.; Sexton, P. M.; Christopoulos, A. Critical role for the second extracellular loop in the binding of both orthosteric and allosteric G protein-coupled receptor ligands. *J. Biol. Chem.* **2007**, *282*, 25677–25686.
(62) Klco, J. M.; Wiegand, C. B.; Narzinski, K.; Baranski, T. J. Essential role for the second extracellular loop in C5a receptor activation. *Nat. Struct. Mol. Biol.* **2005**, *12*, 320–326.
(63) Scarselli, M.; Li, B.; Kim, S. K.; Wess, J. Multiple residues in the second extracellular loop are critical for M3 muscarinic acetylcholine receptor activation. *J. Biol. Chem.* **2007**, *282*, 7385–7396.
(64) Cotte, N.; Balestre, M. N.; Phalipou, S.; Hibert, M.; Manning, M.; Barberis, C.; Mouillac, B. Identification of residues responsible for the selective binding of peptide antagonists and agonists in the V2 vasopressin receptor. *J. Biol. Chem.* **1998**, *273*, 29462–29468.
(65) Jäger, D.; Schmalenbach, C.; Prilla, S.; Schrobang, J.; Kebig, A.; Sennwitz, M.; Heller, E.; Tränkle, C.; Holzgrabe, U.; Höltje, H. D.; Mohr, K. Allosteric small molecules unveil a role of an extracellular E2/transmembrane helix 7 junction for G protein-coupled receptor activation. *J. Biol. Chem.* **2007**, *282*, 34968–34976.
(66) von Kügelgen, I.; Wetter, A. Molecular pharmacology of P2Y-receptors. *Naunyn-Schmiedeberg's Arch. Pharmacol.* **2000**, *362*, 310–323.
(67) Costanzi, S.; Mamedova, L.; Gao, Z. G.; Jacobson, K. A. Architecture of P2Y nucleotide receptors: structural comparison based on sequence analysis, mutagenesis, and homology modeling. *J. Med. Chem.* **2004**, *47*, 5393–5404.

JM801442P